國　立　交　通　大　學

機械工程學系

碩士論文

Experimental and Numerical Investigation of N_2O Flow Feeding System in a Hybrid Rocket

混合式火箭內 N_2O 流體供應系統實驗及模擬之研究

研究生：莊康旻

指導教授：吳宗信 博士

中華民國一百零一年八月

混合式火箭內 N_2O 流體供應系統實驗及模擬之研究

Experimental and Numerical Investigation of N_2O Flow Feeding System in a Hybrid Rocket

研 究 生：莊康旻　　Student：Kang-Ming Chuang

指導教授：吳宗信　博士　　Advisor：Dr. Jong-Shinn Wu

國立交通大學

機械工程學系

碩 士 論 文

A Thesis

Submitted to Institute of Mechanical Engineering

College of Engineering

National Chiao Tung University

in Partial Fulfillment of the Requirements

for the Degree of

Master of Science

In

Mechanical Engineering

August 2012

Hisnchu, Taiwan

西元 2012 年 8 月

混合式火箭內 N_2O 流體供應系統實驗及模擬之研究

學生：莊康旻　　指導教授：吳宗信博士

交通大學 機械工程學系

摘要

混合式火箭近年來受到高度關切，不僅僅因為其得以控制推力的優點，更因為環保無汙染，並且操作較為安全。為了善用推力控制，最容易的方法為控制進入燃燒室之氧化劑之質量流率。本論文旨在探討一利用文氏管校正及量測之流量系統，能使用氧化亞氮或二氧化碳作為操作流體，並且可以 HBMS 真實流體模擬，與實驗結果相互比較。並且利用白努利定律假設流體為不可壓縮流體導出經驗公式，探討文氏管入口及喉管壓力差及質量流率之關係，求得一經驗係數(C_v)。

此一使用氧化亞氮之文氏管校正及量測之流量系統，包含可使用氮氣加壓之儲存槽，可調整壓力範圍目前為 63 至 85 大氣壓，能使用氧化亞氮或二氧化碳作為操作流體，並且在出口處安置一直徑 7 毫米之孔板(orifice)，藉由孔板之背壓控制文氏管下游壓力。此論文使用二氧化碳取代氧化亞氮為實驗流體，因為兩者熱力學性質相似，且二氧化氮價格便宜甚多。最後完成三種文氏管設計，入口內徑分別為 10、28 及 28 毫米，喉管直徑分別為 8、16 及 20 毫米，量測質量流率範圍分別在 1~2、3~8、6~12 公斤/每秒。壓力計及熱電偶安置其內分別量測即時壓力及溫度。實驗平台使用荷重元量測儲存槽內流體即時重量變化，用以推斷各時間點之質量流率。

現階段結果顯示模擬與實驗量測得之數據非常接近，並且根據前段描述之三種不同流量範圍量測用之文氏管，以白努利定律推導出之不可壓縮流之經驗係數(C_v)分別為 0.96、0.97 及 0.91。建議及未來展望也會在此論文結尾作討論。

Experimental and Numerical Investigation of N_2O Flow Feeding System in a Hybrid Rocket

Student : K. M. Chuang Advisor : Dr. J. S. Wu

Department of Mechanical Engineering

National Chiao-Tung University

Abstract

Hybrid rocket propulsion has attracted much attention recently mainly because of its capability of thrust profiling, in addition to its safe and green operation. To realize thrust control, the easiest way is to accurately control the flow rate of oxidizer flowing into the combustion chamber. In this thesis, a venturi flow meter calibration/measurement system for pressurized nitrous oxide or carbon dioxide is developed and validated by comparing between experiments and flow simulations using real-fluid HMBS model. An incompressible Bernoulli type empirical correlation that links between pressure difference (inlet and throat) and mass flow rate is also proposed with an empirical coefficient.

This venturi flow meter calibration/measurement system for nitrous oxide includes a nitrogen pressurized source tank with adjustable pressure (63-85 bars), a venturi flow tube and an orifice (7 mm in diameter) for controlling the back pressure in the downstream of flow meter. CO_2 is used as the working gas in this thesis instead of N_2O because of their similarity in thermodynamic behavior and also large cost saving. Three different venturi flow tubes, including 10, 28 and 28 mm in inlet diameter with 8, 16 and 20 mm in throat diameter, respectively, were designed to

cover different ranges of mass flow rates, including 1~2, 3~8, 6~12 kg/s, respectively. Pressure transducers and themocouples were used to measure instantaneous pressure and temperature, respectively, wherever is necessary. A load cell is used to measure the instantaneous weight of the pressurized tank during experiment that can be used to deduce the instantaneous mass flow rate.

Results show that the simulations agree very well with the measurements performed in the current study. An empirical correlation based on the incompressible Bernoulli type equation is proposed with velocity coefficients of 0.96, 0.97, and 0.91, respectively, for the three ranges of flow rates as mentioned in the above. Recommendations for future work are also outlined at the end of the thesis.

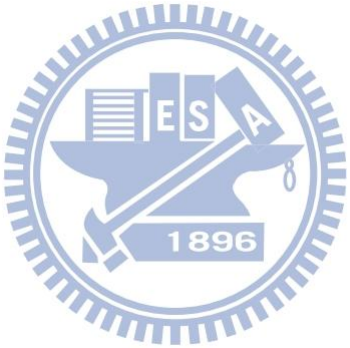

誌謝

我對這實驗室的印象不是只有短短兩年碩士,卻是吳宗信老師自大學三年級就開始的栽培教導。不但從火箭計畫的執行中學會不少寶貴的處事經驗,也因為幾次的國際會議以及各種會議場合報告,學習到許多與人溝通所必須要有的邏輯思考能力、對數字小心謹慎的態度,以及最重要的,待人待科學所保持的誠信原則,在實驗室兩年的日子,受益良多且讓我感慨到,有朝一日一飯千金的恩情得好好回報!

實驗室相處是幾乎感覺不到壓迫的氛圍,在假日空閒之餘還能偶爾大家一同到竹南海邊享受大自然波浪力學的威力,平常在實驗室內卻也能嚴謹的互相幫忙,把事情做到最好。動靜自如的學生生涯,讓我能慶幸當年選擇多留在交大兩年,了解自己所喜歡的學習過程,並且在最後努力的完成這分論文。

這分論文的完成並不只有我的功勞,還得感謝太空中心陳彥升博士、來自美國的客座教授鄭智雄老師、學長周子豪、古必任、賴冠融以及學弟林哲緯,在這篇論文不論是實驗或是模擬,提供了許多精彩寶貴的意見及方法,實驗室豐富的資源也讓我從來沒有為研究過程中的經費設備需要煩惱分毫,這樣的環境能讓我不斷提醒自己,缺少的是尚有很大進步空間能力。

也很感謝國科會計畫的支持,計畫編號: NSC99-2221-E-009-056-MY2

最後且最鄭重感激的是我的家人,父母的支持讓我沒有後顧之憂的盡情飽覽學術殿堂的宏偉,我諸位家人所冀求的,只是完成子女們的夢想,不待任何偏見的無私奉獻支持,才讓我能走到今天這個段落。

我一定會回來看到劃台灣歷史新指標的火箭發射,也希望有朝一日這個地方能夠不僅僅是我,而是台灣全國人民的驕傲。

康旻 謹致

2012 年 8 月于風城交大

Table of Contents

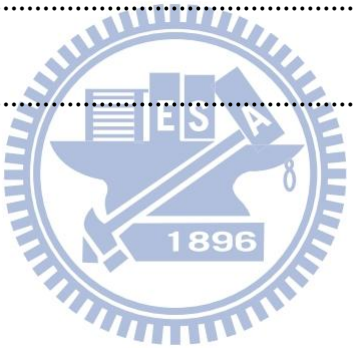

List of Tables

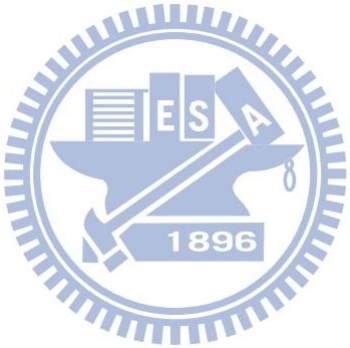

List of Figures

Nomenclature

ρ	:	liquid density, kg/m^3
D	:	venturi inlet diameter, mm
d	:	venturi throat diameter, mm
ΔP	:	pressure difference between inlet and throat, bar
$\dot{m}$	:	Mass flow rate, kg/s
C_v	:	Velocity coefficient
A_1	:	Venturi inlet area, m^3
A_2	:	Venturi throat area, m^3
P1	:	Venturi inlet pressure, bar
P2	:	Venturi throat pressure, bar
P3	:	Venturi downstream pressure, bar
T1	:	Venturi inlet temperature, ℃
T2	:	Venturi throat temperature, ℃
T3	:	Venturi downstream temperature, ℃
P_{12}	:	pressure difference between inlet and throat, bar
P_{13}	:	pressure loss, pressure difference between inlet and downstream, bar
PT	:	Pressure in the tank, bar

Chapter 1 Introduction

1.1 Background and Motivation

1.1.1 Hybrid Rocket System

The idea of hybrid rocket first mentioned in 1930, and development of this field is still improving until these years, new methods and materials kept discovered. The idea of using nitrous oxide (N_2O) as a rocket propellant can be traced back to the beginning of 20^{th} century, when famous American rocket scientist Robert H. Goddard proposed using N_2O in rocket propellant as an oxidizer and gasoline as fuel [1]. Until contemporary rocket technology, N_2O has been widely used as oxidizer in hybrid propulsion, it reveals research in this area still has considerable amount of potential in many area include academia research and commercial use. As Fig. 1-1 shows, in 2004, Space Ship One spacecraft launched from Mojave Aerospace Ventures, and successfully let 3 pilots reached 100 km altitude, and won the Ansari X Prize. Also in Fig. 1-2 shows British private group Bloodhound SSC applied hybrid rocket engine in a hybrid car and reach mach number 1.4 when it's racing on the ground. All these facts show that hybrid propulsion using N_2O is still developed by other enterprises, academic units or amateur interest groups.

Fig. 1-3 shows three typical rocket propulsion systems, solid, liquid, and hybrid propulsion system. With solid propellant as fuel and liquid propellant as oxidizer,

hybrid propulsion process throttling or shutdown capability which solid propulsion cannot make it once it ignited. And building a hybrid rocket system is less complexity than a liquid propulsion system.

Commonly used hybrid propulsion systems oxidizers are nitrogen tetra oxide (N_2O_4), hydrogen peroxide (H_2O_2), liquid oxygen (LOX), or nitrous oxide (N_2O). Hybrid propulsion using N_2O as oxidizer possesses couple advantages. First, it's non-toxic unlike nitrogen N_2O_4 or H_2O_2, which has also been used as hybrid propellant but poisonous. Second, it's easier to store in room temperature unlike liquid oxygen which needs to keep in low temperature to remain liquid phase. Easier handling process reduced the cost of storing N_2O. Last but not least, its saturated liquid pressure at room temperature makes it an ideal self-pressurizing oxidizer (57.3 atm at 293.1 K). Therefore, compare to other high performance and common used oxidizers, N_2O is environmentally green with its non-toxic property, easier to store with saturated stable in room temperature, and easier to utilize as its self-pressurizing characteristics.

As we mentioned above, the throttling-capability is a feature of hybrid propulsion system. Either by controlling the control valve opening angle or by changing helium pressure, the flow rate of high pressure oxidizer varies. Thus the throttling control can be performed by manipulating N_2O mass flow rate.

1.1.2 Fluid Properties of N_2O and CO_2

Nitrous oxide seemed to be a perfect oxidizer as hybrid rocket propellant. However, there's also disadvantage while manipulating N_2O. Its supercritical multiphase cannot be precisely predicted by considering it as ideal gas, compressible fluid, nor incompressible fluid. The multiphase characteristic required Real-fluid model to perform simulation with multiphase supercritical fluid like N_2O or carbon dioxide (CO_2). CO_2 cannot be used as rocket propellant. As Fig. 1-5 and Fig. 1-6 shows, it's thermal properties under saturated liquid state is highly similar to N_2O, With the approximately and 10 times cheaper cost, CO_2 is a great choice as a substitution for N_2O.

1.1.3 Types of Flow Meters for High Pressure Flow Conditions

There are already several types of industrial standard flow meter existed, but most of them cannot adequately meet the needs of measuring the fluid pass through the meters in this case.

The fluid working environment for liquid oxidizer has several requirements that are differ to any designed industrial products. First, it is under a range of temperature change from room temperature to -20 ℃. Second, the whole system might vibrate severely during flight test, and the gravitational force in flow meter will change. Third, mass flow rate in the meter is high with range between 1 kilogram per second to 10 kilogram per second. Last but not least, not only fluid is in high pressure while

entering the flow meter, it also has to keep the fluid maintain high pressure, in other words, the flow meter cannot cause high pressure loss during measuring in order to provide high mass flow rate in combustion chamber.

There are some reasonable flow meters been tested by NASA, some of them failed in useless, some of them caused hazardous disaster. Fig. 1-7 shows turbine flow meters and vortex shedders seems legit. However, as record showed, any moving mechanism in the oxidizer or any friction heat caused by metal material in flow meter will cause lethal explosion.

Under such circumstances, pressure difference flow meters seemed to be better choice. Fig. 1-8 shows There are several kinds of pressure difference flow meters, but their Performance differs a lot , as Fig. 1-9 shows. Orifice plate seems ideal, but the downstream pressure will drop at least 30 percent. So it turns out a venturi meter with converging and diverging part for pressure recovery and no moving mechanism is ideal by measuring pressure difference to get the mass flow rate.

However, venturi flow meter has to be calibrated in different flow condition with different cases, so it’s impossible to find suitable industrial product for unique hybrid rocket propulsion.

1.1.4 Venturi Flow Meters

With such special flow condition in hybrid propulsion system, self designed venturi flow meter is a better solution for measuring mass flow rate. A typical venturi

flow meter consists of an upstream inlet pipe region with certain angle of slope shape, a throat region, pressure will drop at throat region while flow velocity reaches the highest at throat region, a slope for pressure recovery to downstream region, and it should be less steep than upstream slopes.

Roughly calculated with Bernoulli equation, the oxidizer passing through the venturi flow meter can be expressed as below :

$$\dot{m}_{ox} = C_v A_2 \sqrt{\frac{2\rho_{ox}\Delta P}{1-(\frac{A_2}{A_1})^2}} \quad (1)$$

With the inlet area and throat area represented as A_1 and A_2, respectively. The venturi flow meter was calibrated by experimental data, determined the velocity coefficient, C_v. And the pressure difference between inlet and throat, ΔP. Density of oxidizer is being calculated as function of temperature, ρ_{ox}. We have to conduct several tests to confirm the result and minimize the error.

Industrial venturi flow meter dimension and calibration data are very easy to find in [2]. However, in the beginning paragraph notified it's for single-phase fluid, not for multiphase fluid. Therefore, it will need for calibration with density variation.

1.1.5 Calibrated Bernoulli Equation for Venturi Flow Meters

As mentioned above, thermal properties of N_2O and CO_2 showed the density varies a lot when temperature of oxidizer changes when it flows through flow feeding line, as Fig. 1-10 shows. With this characteristic, mass flow rate equation has to be calibrated as different temperature of fluid flows in fluid.

Thus, as Fig. 1-11 shows, the correlation line will be steeper when the temperature increase, in other words, the density of oxidizer has smaller density.

1.1.6 Literatures Survey

The design in proposed flow feeding system uses a venturi with multiphase high pressure N_2O or CO_2 saturated liquid. The mass flow rate is relatively high compares to other lab scale flow meter because it's needed for the use of HTTP rockets, which is range from 1 ~ 10 kilogram per second. Only a few research topics studied about high pressure and mass flow rate venturi flow meter. Lots of reports took ISO standard as reference for designing a new venturi for multiphase fluid, but results and calibration equations are totally different from the result under single-phase assumptions.

A classical report is in 1970, D.W. Harvey [3], talked about throttling control of LOX fuel in liquid rocket engine, Lunar Module Descent Engine (LMDE). It was an experiment of stoke adjusting of pintle mechanism in a cavitating venturi flow meter. The result discussed about wide range of correlation between pressure difference and mass flow rate. Although its mass flow rate is too high and dimension is very large because it's a LMDE, but it was the very beginning of high pressure liquid propellant using cavitating venturi as a flow meter. Thus, almost all studies of rocket flow meter

afterwards took reference of the paper.

In 2006, A. Ulas [4] proposed a study of cavitating venturi flow meter, with 2 kinds of pressurize during experiment (high pressure gas tank, ignite composite grain) and FLUENT as simulation result to validate it's experiment. It successfully builds a venturi flow meter with cavitating at the throat area, and high pressure water as working fluid. Although the venturi design is working in 10 kilogram per second, it used water as working fluid, the result in N_2O and CO_2 will be totally different. Besides, the cavitating design will make the downstream a huge pressure loss.

In 2006, Kevin Lohner et al. [5] build a lab scale HTPB-N_2O hybrid propulsion system. It uses venturi to measure pressurized N_2O liquid oxidizer. Although the whole hybrid propulsion system is the same as HTTP rockets and the designed venturi measured N_2O in liquid phase, the drawback of built system is it is a lab scale 0.06 kg/s mass flow rate rocket engine, in which doesn't fit the requirement of 1~10 kg/s mass flow rate for HTTP hybrid rockets. But is a very good experimental result as benchmarking for our Real-fluid simulation code.

1.1.7 Overview

Therefore, after literatures surveyed, we found that the fluid condition in our case haven't been researched. Those related literatures can't meet our need of building a

high-mass-flow-rate flow feeding system. Thus, we need to build a flow system in this thesis.

1.1.8 Motivation

So far we understand that hybrid rocket can be capable of throttling control by means of measuring its mass flow rate. And the whole flow feeding system can be experimented and simulated. However, existed studies are so insufficient because the flow feeding system is working at high mass flow rate, high pressure, and N_2O real fluid. Therefore, to perform throttling control for hybrid rocket, it is needed to build up a flow feeding system that mass flow rate can be measured.

1.2 Specific Objectives of the Thesis

After above literature surveyed, we found that research of venturi flow meter using high pressure multiphase liquid under high mass flow rate is pretty rare, especially when using nitrous oxide as working fluid, both experiment and simulation cannot find enough research data using nitrous oxide liquid in venturi flow meters. Thus, for the goal of performing throttling control in HTPB-N_2O hybrid propulsion system, we need to build up a flow feeding system to measure the flow condition.

Therefore, in this thesis, we build up a flow feeding system with such objectives:

1. A flow feeding system with flow meter. 2. The working fluid should be stable, non-cavitating flow. 3. I have to be able to serve high mass flow rate (1~10 kg/s), using CO_2/N_2O high pressure liquid as working fluid. 4. Few sets of venturi flow meters for measuring pressure difference (1~10 bar), and pressure at downstream cannot drops below 40 bar for the need of combustion chamber. 3. A well developed simulation tool for non-ideal gas but real-fluid simulation, being able of simulating mass flow rates for N_2O/CO_2 real-fluid for the need of designing better venturi flow meter.

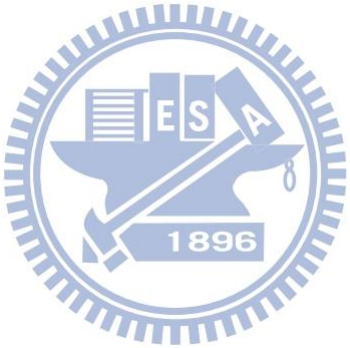

Chapter 2 Numerical Method

In this thesis, we use the UNIC-UNS code, developed by Y.S. Chen et al, to simulate an unsteady compressible flow. It uses Navier-Stokes solver with finite volume method. The governing equation, boundary condition, numerical methods, algorithm and so on will be discussed below.

2.1 Governing Equations

The general form of mass conservation, energy conservation, Navier-Stokes equation and other transport equations can be written in Cartesian tensor form:

$$\frac{\partial(\rho\phi)}{\partial t}+\frac{\partial}{\partial x_j}\left(\rho U_j\phi\right)=\frac{\partial}{\partial x_j}\left(\mu_\phi\frac{\partial\phi}{\partial x_j}\right)+S_\phi \qquad (1)$$

where μ_ϕ is an effective diffusion coefficient, S_ϕ denotes the source term, ρ is the fluid density and ϕ = (1, *u*, *v*, *w*, *h*, k, ε) stands for the variables for the mass, momentum, total energy and turbulence equation, respectively.

2.2 Real-Fluid Modeling

The idea of real fluid model first proposed by van der Waals in 1873, considering the limitation in the equation of state of ideal gas are: high pressure, low temperature, and phase change, in which molecules would interact with each other, van der Waal

build up a model give a closer approximation to real fluid situation.

In 1958, HBMS [6] real fluid model fixed and optimized van der Waal's model, gave a better approaching to real fluid, which considered phase change in different equation of state.

Furthermore, to apply the HBMS model, there's 2 ways to implement its properties into CFD: 1. Directly solve the equation of state in the model 2. Using table look-up method. Although solving the equation is more accurately, it is also time consuming for huge loading of computer calculations. Thus, in this study, we use table look-up method in order to save 60% of calculation times. Fig.2-2 shows a built up table.

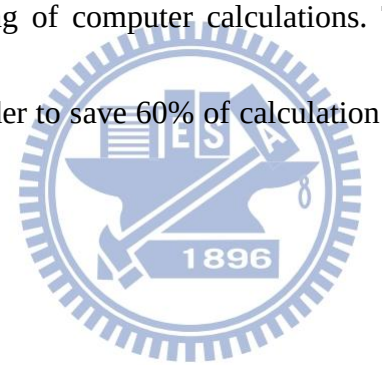

Chapter 3 Experimental Method

3.1 Experimental Facility

The whole experiment pipe and instruments diagram are in Fig. 3-1. We can operate the whole flow feeding system with an adequate standard operation procedure with such detail description of all valves and sensors. The flow feeding system consists of 4 modes : filling mode, pressurizing mode, stand-by mode, and run mode. All 4 modes condition and operation detail will describe in detail in 3.3, test procedures.

3.1.1 High-Pressure Liquid Supply Source Stand

As it mentioned in the background, we use CO_2 as experimental fluid first, there's also a helium pressurize apparatus to adjust to the high pressure as we required.

3.2 Experimental Instrumentation

The whole experimental instruments sketch is in Fig. 3-1. With 4 pressure transducers, 2 thermocouples, 1 differential pressure transducers and 1 load cell data will be processed in a National Instruments data acquisition system.

By these data, we can understand pressure from tank, venturi upstream, venturi

throat, and venturi downstream. And differential pressure transducer will obtain pressure difference directly from upstream and throat. Also, by load cell data, we can know mass flow rate as function of time to correlate the data with pressure difference measured from venturi flow meter.

3.2.1 High Frequency Pressure Transducer

The pressure transducers (JETEC JPT-131) in the experimental rig have 100 Hz frequency, with range of 100 bar, error at 2.5% in full scale. 4 transducers record down the pressure data from tank, venturi upstream, venturi throat, and venturi downstream. But we cannot use the data to obtain pressure difference because its error is too high to resolute the accurate pressure difference value, so that is why we need differential pressure transducer.

3.2.2 Differential Pressure Transducer for Pressure Change Measurement

Differential pressure transducer (NPXD-10-N-K) in use for the experiment has maximum 10 bar, full scale error at 2.5%. Tapping location at upstream and throat of venturi meter.

3.2.3 Thermocouples for Temperature Measurement

T-type thermocouple utilized in the experiment, range from -200 ℃ to 350 ℃. Probe diameter is 1.6mm. By the temperature we measured, we can calculate the vapor pressure at certain time, and understand whether the fluid in the system vaporized or not.

3.2.4 Load Cell for Mass Flow Measurement

The whole tank located on a test stand with s-beam load cell installed under the test stand, with range of 250 kg, 0.1 kg error. Also, by load cell data, we can know mass flow rate as function of time to correlate the data with pressure difference measured from venturi flow meter.

3.3 Test Procedures

After all apparatus and instruments set up. First thing to do is filling N_2O/CO_2, the source tank must filled with N_2O/CO_2 liquid with nitrogen pressurized over saturation pressure of N_2O and CO_2, which is 51 atm for CO_2 and 53 atm for N_2O. To begin the filling process, in Fig. 3-3 shows, first step is filling mode, filling valve is opened, experiment valve is closed, and venting valve is opened to make sure it's filled with the most N_2O/CO_2 it can be, otherwise the whole filling process will stop

when source tank reached saturation pressure due to vaporization inside source tank. After the source tank reached the desired liquid weight, the pressurizing valve is opened to perform pressurizing mode as Fig. 3-4 shows. Then N_2 fill in the N_2O/CO_2 vapor gas space in source tank, pressurized the liquid existed in the tank until it reached the pressure the experiment need for certain upstream pressure and mass flow rate. After the pressurization process complete, close the pressurization valve, open the stand-by valve to fill the whole venturi with N_2O/CO_2 liquid, and then open the venturi exhaust valve to exhaust gas in the venturi, and remove the filling CO_2/N_2O tank and open the filling valve to exhaust gas in the pipe as Fig. 3-5 shows. After all these procedure done, the blow down experiment is ready, using the electro-magnetic valve to start the experiment as Fig. 3-6 shows. Once an experiment done, stand-by valve need to close first to prevent if sudden close for the experiment valve, an unwilling shock wave could damage transducers.

Chapter 4 Results and Discussion

4.1 Validations

To validate the real fluid simulation code, venturi design in the case as surveyed literature [5] is used as benchmarking. We build up a model in which geometry is same as the venturi designed in the paper [5] and shows in Fig. 4-1. Then using the experimental data in comparison with our simulation tool, and result shows in Fig. 4-2.

Simulation results show the pressure difference in the mass flow condition (0.063 kg/s) in the paper is 1.09 bar, whereas the experimental result is 1.08 bar. The simulation result show the code is reliable for the use of design a new venturi.

4.2 Simulation Conditions

An axial symmetric grid with different expand angle for the throat in venturi has been build up, throat diameter, pipe length, and different pipe diameter to get the optimized design.

In the fluid conditions, we fix different upstream mass flow rate sets, with downstream mass conservation, and the initial pressure is set as 69 bar, same as pressurized conditions.

4.3 Simulation Experimental Results

4.3.1 Simulation Results

Fig. 4-5 shows a 10 mm venturi with different throat diameter and different expand angle. We can realize expand angle difference doesn't influence the pressure difference much, what really matter should be throat diameter, and 8mm throat is a better choice, because the pressure difference between 1 to 2 kg/s mass flow rate is range from 2 to 7 bar, which is better for sensor working. And the result shows downstream pressure drops over 8 bar when mass flow rate reach 3 kg/s, which is too much pressure loss, so the 10 mm design has mass flow rate limit for 2 kg/s.

In Fig. 4-6, we tried to extend the pipe length and found that with longer venturi overall length, the pressure difference range will be larger along mass flow rate variation, so we picked the longer venturi design, and using CO_2 for another simulation result as shown in the figure.

In Fig. 4-7 shows, after confirming the simulation result with CO_2, then using the density value when temperature is 295 K (22℃) and the Bernoulli equation for the calculated result, found out the velocity coefficient C_v has to be 0.96 to match the simulation result.

After confirming the design for 1~2 kg/s mass flow rate, we design 3 mor venturi

with larger diameter. With 28 mm diameter, we tried throat diameter for 16 mm, 20 mm, 22 mm. The simulation results shows in Fig. 4-8. And we can found that in venturi with 22 mm throat diameter has too low pressure difference when mass flow rate change. So we picked 2 venturi sets as our final design in Fig. 4-9, which are throat 16mm, and 20mm for mass flow rate at range 3~8 kg/s and 6~12 kg/s, respectively. Also, because the system can work on mass flow rate under 3.7 kg/s, so there's also a result for 16 mm throat diameter shows CO_2 mass flow rate under 3.7 kg/s.

To sum up, for the above simulation, we designed 3 sets of venturi design can be used for mass flow rate ranging from 1~12 kg/s. As Fig. 4-10 shows, 2 venturi pipes are simulated with CO_2 mass flow rate below 4 kg/s.

4.3.2 Experimental Results

Until now, we have done 5 successful experiments with few seconds of N_2O with fully liquid phase inside the flow feeding system had been performed. Case 1 is done by 10 mm venturi flow meter installed, case 2~5 is with 28 mm diameter venturi with throat diameter of 16 mm. Case 2 and 3 did not install orifice. The detailed experiment condition can be viewed at *Tank pressure as test starts

†Case #2 and #3 does not have orifice installed

Table 4-1.

The measured data in pressure transducers is in Fig. 4-11, and load cell and upstream thermocouple data T1 is in Fig. 4-12. We need to arrange these data, calculating pressure drop P_{13} by differentiating P1 and P3, obtaining upstream vapor pressure by T1, and derivative load cell data along with time to get mass flow rate. These data shows in Fig. 4-13 and Fig. 4-14.

After above pressure, mass flow rate, and differential pressures obtained, we combined data with the figure like in Fig. 4-15. Then we can know time as function of pressure, mass flow rate, P_{13} and P_{12}. Then we can understand what happened in each period of time and define the useful data region. In region A, the whole system is stand by. In region B, huge pressure drop in the beginning of the experiment. In region C, the whole venturi is filled with flowing liquid, all pressure drops in certain rate, mass flow rate almost remain constant. When it goes to region D, rising up of P_{13} reveals that downstream happened pressure loss due to vaporization, and it will also influences the throat region, made the pressure difference value less accurate as correlation for mass flow rate. Then in region E, the turning slope of P1 means that all liquid in the tank exhausted, only vapor in venturi tubes. Thus, case 2~5 shows in Fig. 4-16, Fig. 4-17, Fig. 4-18 and Fig. 4-19,respectively, with all 5 regions defined. And in Fig. 4-20 comparison of P1 and PT trend as function of time for case 3 and case 5,

we can understand case 3 occur almost 20 bar pressure drop in the beginning, compare to only drops 7 bar in case 5, prove that flow feeding line with orifice will avoid too huge pressure drop in the beginning.

4.4 Empirical Correlation

From Fig. 4-21 we can see that result in 10 mm venturi pipe the case 1 result match the pressure difference range in 5 ℃, so we redo the simulation with different temperature and theory line in different density due to temperature drop to understand the relation of result change. And we can find out that the experimental result in case 1 lies in the simulation curve and correlated theory curve.

In Fig. 4-22, we can see results from case 2 to case 5, all 4 cases for experimental result lies near the simulated line, with these result, we can conclude that by developing a theory line of venturi performance by calibrating Bernoulli equation, we can have a prediction for mass flow rate in the flow feeding system.

4.5 Recommended Final Designs

From the experimental and simulation result along with correlation by Bernoulli equation, conclusion is that 3 kinds of venturi flow meter are done. 10, 28 and 28 mm in inlet diameter with 8, 16 and 20 mm in throat diameter, respectively, were designed

to cover different ranges of mass flow rates, including 1~2, 3~8, 6~12 kg/s, respectively.

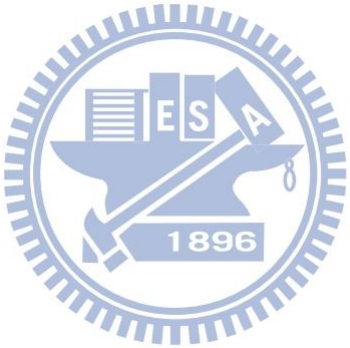

Chapter 5 Conclusion and Recommendations of Future Work

5.1 Summary

In this thesis, we have developed and validated a venturi flow meter calibration/measurement system for nitrous oxide. Flow simulations using real-fluid model of nitrous oxide and carbon dioxide were performed and compared with the measurements. An incompressible Bernoulli type equation is used to correlate the experimental mass flow rates as a function of pressure difference between pressures at inlet and throat of the venturi flow tube.

In general, major achievements and findings are summarized as follows:

1. An experimental system for measuring mass flow rates of nitrous oxide through a venturi flow tube has been constructed and tested for various flow rates in the range of 1-12 kg/s.
2. A comprehensive HBMS model has been developed for the real fluid simulations of N_2O and CO_2 and the results of CO_2 was found to agree very well with the measurements.
3. Generally, differential pressure between inlet and throat increases with increasing mass flow rates.
4. Three different venturi flow tubes, including 10, 28 and 28 mm in inlet diameter

with 8, 16 and 20 mm in throat diameter, respectively, were designed to cover different ranges of mass flow rates, including 1~2, 3~8, 6~12 kg/s, respectively.

5. An empirical correlation based on the incompressible Bernoulli type equation is proposed with velocity coefficients of 0.96, 0.97, and 0.91, respectively, for the three ranges of flow rates as mentioned in the above. This shows that the friction loss and real-fluid effect are significant at larger flow rates and is relatively unimportant at smaller flow rates.

5.2 Recommendations of Future Work

Based on the preliminary study in the current thesis, several future directions of research are proposed as follows:

1. To enlarge the diameter of the plumbing tubes for reducing the pressure loss.
2. To repeat measurements of CO_2 by changing the orifice diameter at the exhausting location and the measurements of CO_2 which were not included in the current thesis.
3. To perform critical measurements of N_2O for future realistic applications.
4. To study experimentally and numerically using a multiple-hole orifice plate as the flow meter for CO_2 and N_2O that has a comparable pressure loss as a

compared to venturi flow tube and much smaller space requirement, which are both important in liquid and hybrid rocket propulsion system in practice.

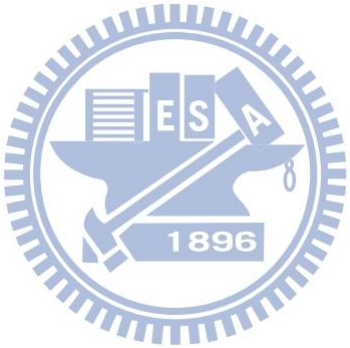

References

[1] Goddard, R. H., “Rocket Apparatus,” US Patent No. 1,103,503 ,191414, 1914

[2] British Standard, “Measurement of fluid flow by means of pressure differential devices”, ISO-5167-4, Part4: Venturi tubes, Second edition, 1991

[3] Harvey, D.W., ”Throttling venturi valves for liquid rocket engines”, AIAA Paper, 1970-703, 1970

[4] Ulas, A. “Passive flow control in liquid-propellant rocket engines with cavitating venturi”, Flow Measurement and Instrumentation, Volume 17, Pages 93–97 , 2006

[5] Kevin Lohner et al., Fuel Regression Rate Characterization Using a Laboratory Scale Nitrous Oxide Hybrid Propulsion System, American Institute of Aeronautics and Astronautics, 2006

[6] Hirschefelder, J. O., et al., Generalized equation of state for gases and liquids., Ind. Eng. Chem., 375–385., 1958

[7] Richard, C. F., et al., Computational Transport Phenomena for Engineering Analyses, (2009)

[8] COMPOSITES, S., “SPACESHIPONE & WHITE KNIGHT,” http://www.scaled. com/projects/tierone/, 2011

[9] Bloodhound, S. S. C., “Bloodhound supersonic car” http://www.bloodhoundssc.com/, 2010

[10] Welsch & Partner, “Rocket-types”, http://www.welsch.com/, 2008

[11] Engineeringtoolbox, http://www.engineeringtoolbox.com/, 2007

[12] National Institute of Standards and Technology, “Thermo Physical Properties of Fluid Systems”, http://webbook.nist.gov/chemistry/fluid/, 2011

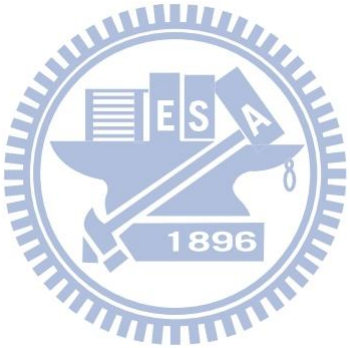

Appendices

Tables

Test Case	Venturi Diameter (mm)	PT* (bar)	Max Mass Flow Rate (kg/s)
C1	10	68	1.78
C2 †	28	78	3.75
C3 †	28	85	3.5
C4	28	69	2.57
C5	28	63	1.97

*Tank pressure as test starts

†Case #2 and #3 does not have orifice installed

Table 4-1 Test conditions

Figures

Fig. 1-1 Manned spaceflight: SpaceShipOne (Mojave Aerospace Ventures, USA; Paul Allen and Scaled Composites, Burt Rutan's aviation company; September 29, 2004) [8]

Fig. 1-2 Hybrid Rocket Car -Bloodhound SSC, UK [9]

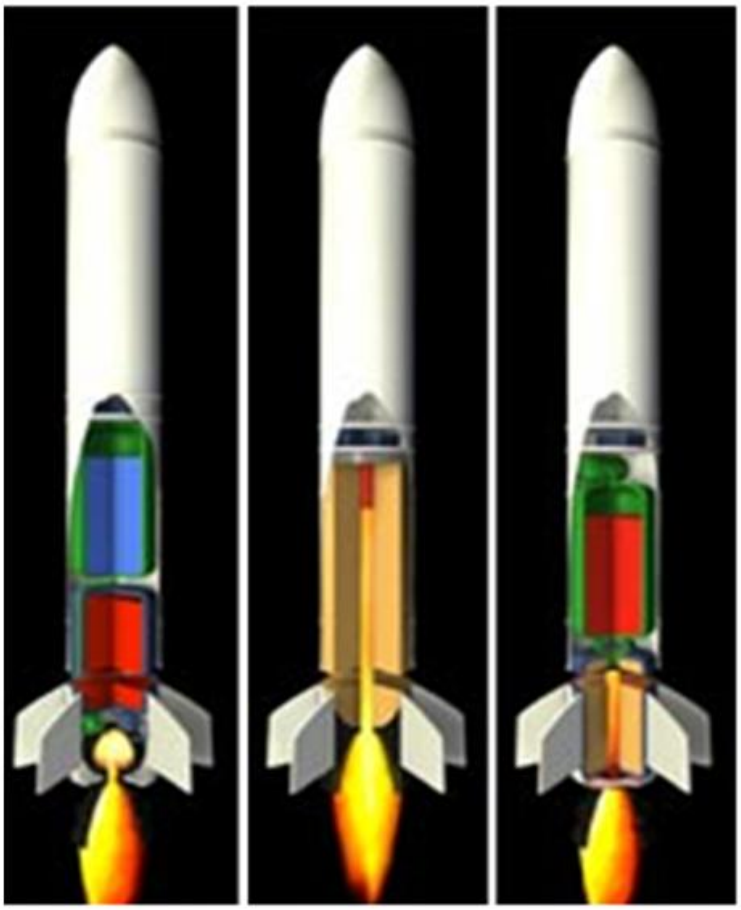

Fig. 1-3 Sketch of typical rocket propulsion systems [10]

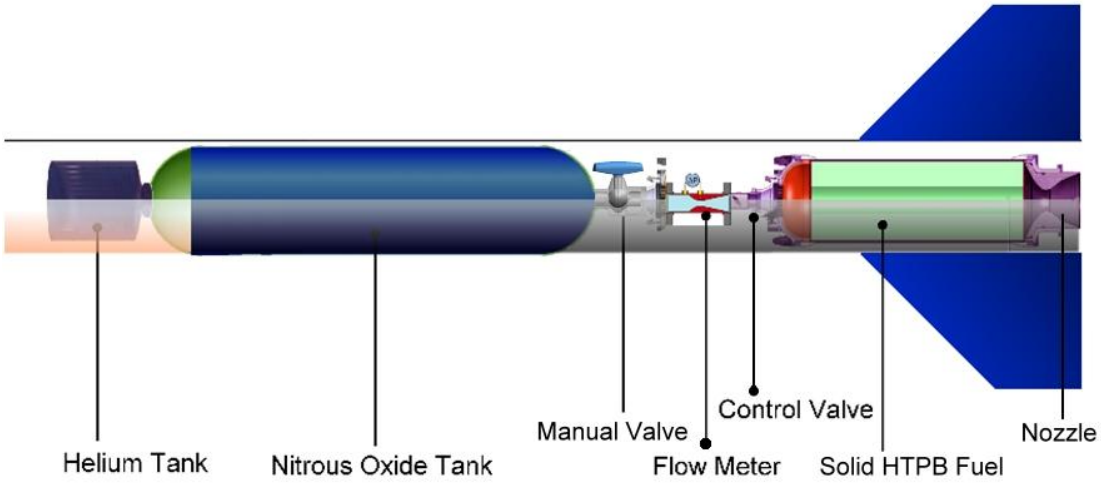

Fig. 1-4 Sketch of typical hybrid propulsion system

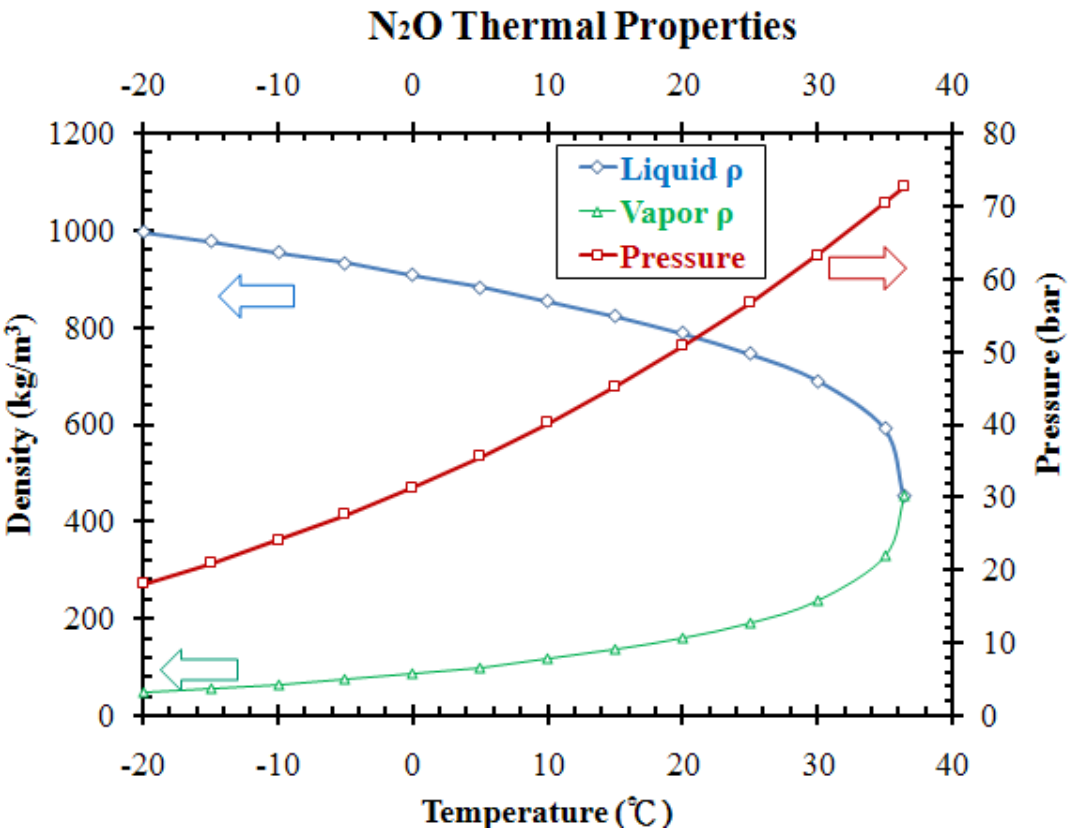

Fig. 1-5 Pressure and fluid density of N_2O as a function of temperature from -20℃ to critical point, 37 ℃ [12]

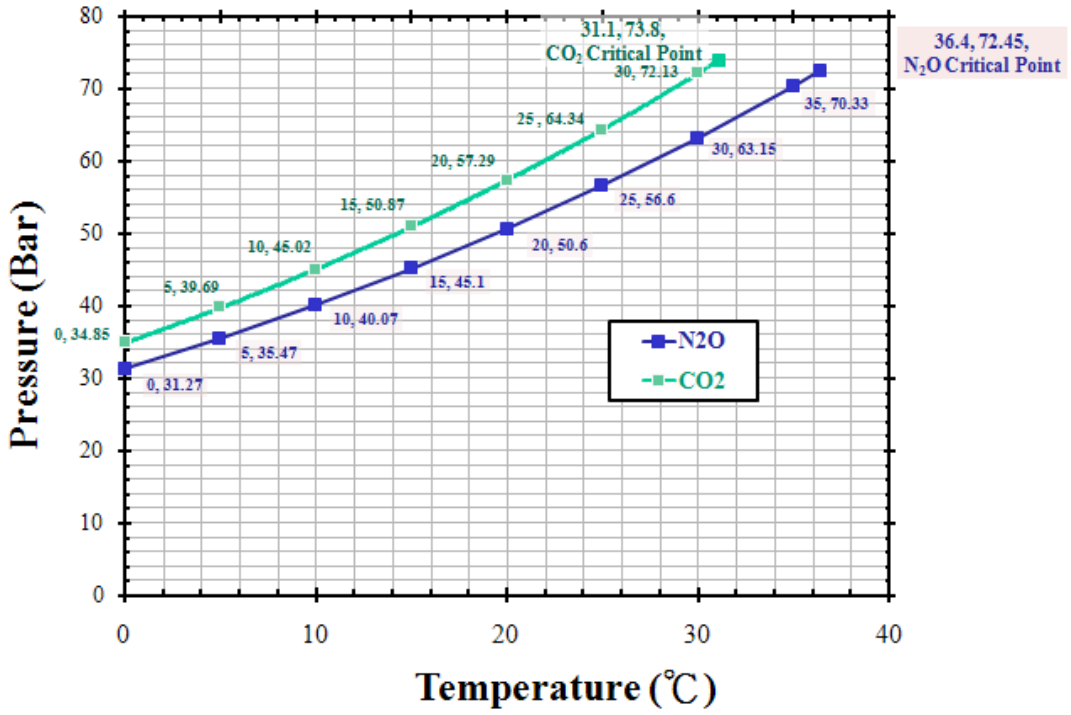

Fig. 1-6 Vapor pressure of N_2O and CO_2 as a function of temperature [12]

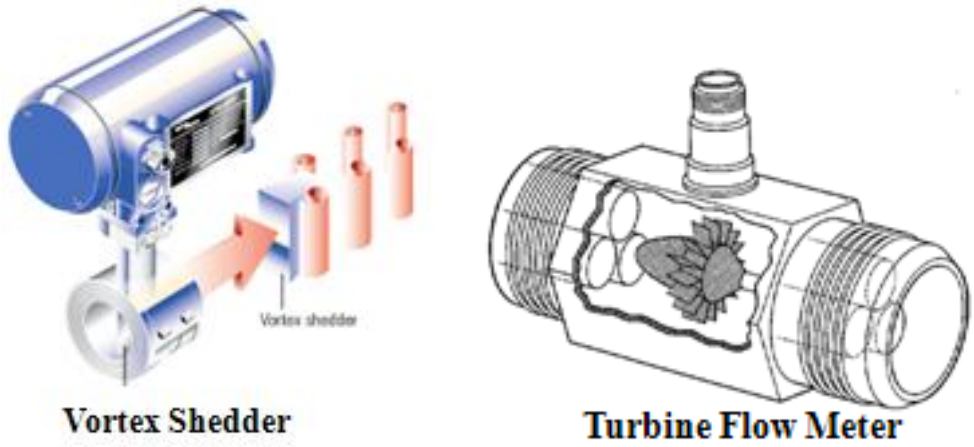

Fig. 1-7 Turbine flow meter and vortex shedder [11]

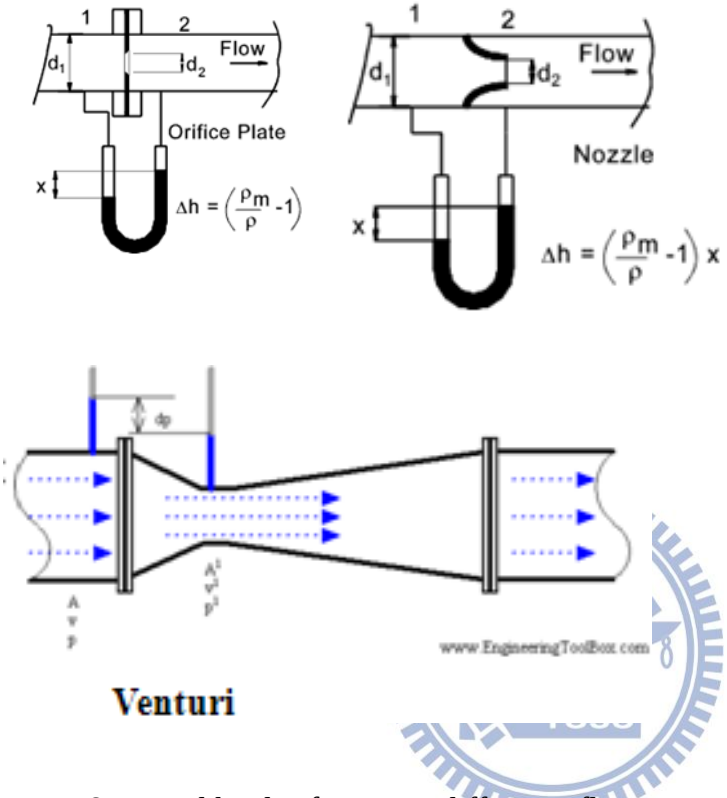

Fig. 1-8 Typical kinds of pressure difference flow meters [11]

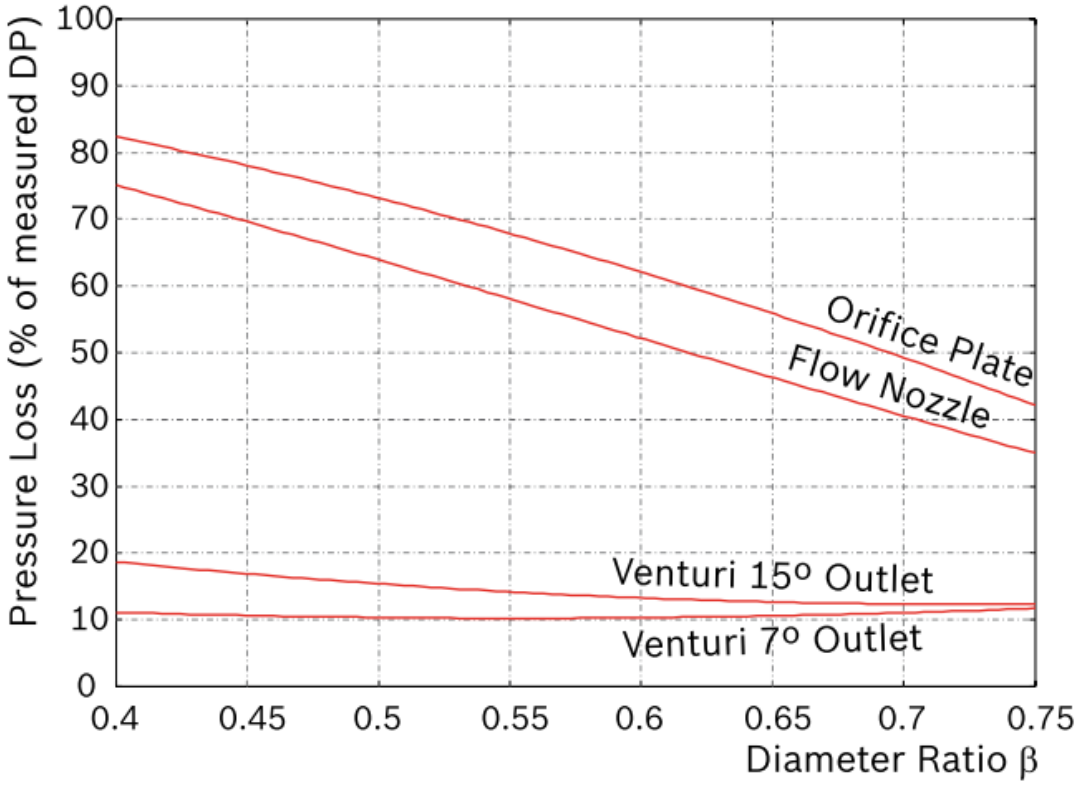

Fig. 1-9 Comparison of pressure loss for couple typical pressure difference flow meters,[11]

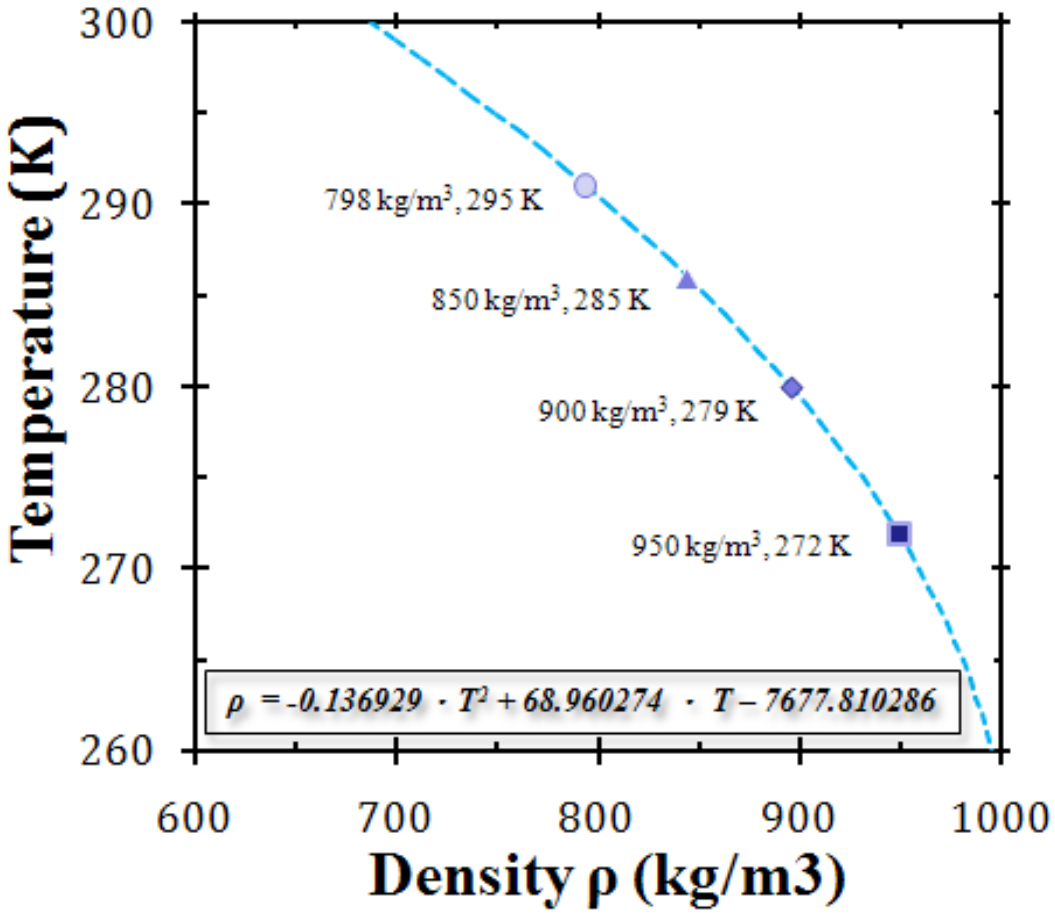

Fig. 1-10 Thermal properties of CO_2, density variation when temperature of oxidizer changes [12]

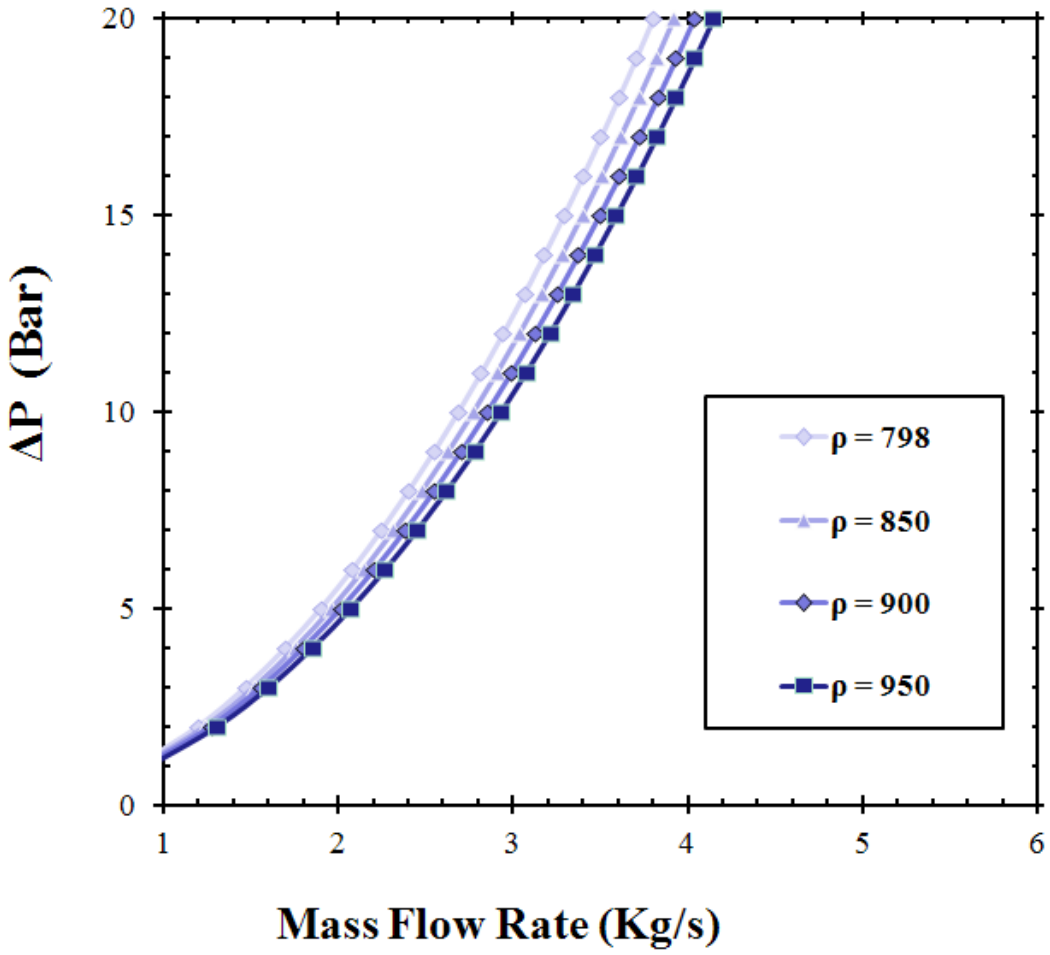

Fig. 1-11 Ideal CO_2 mass flow rate versus pressure difference in a venturi with different density [12]

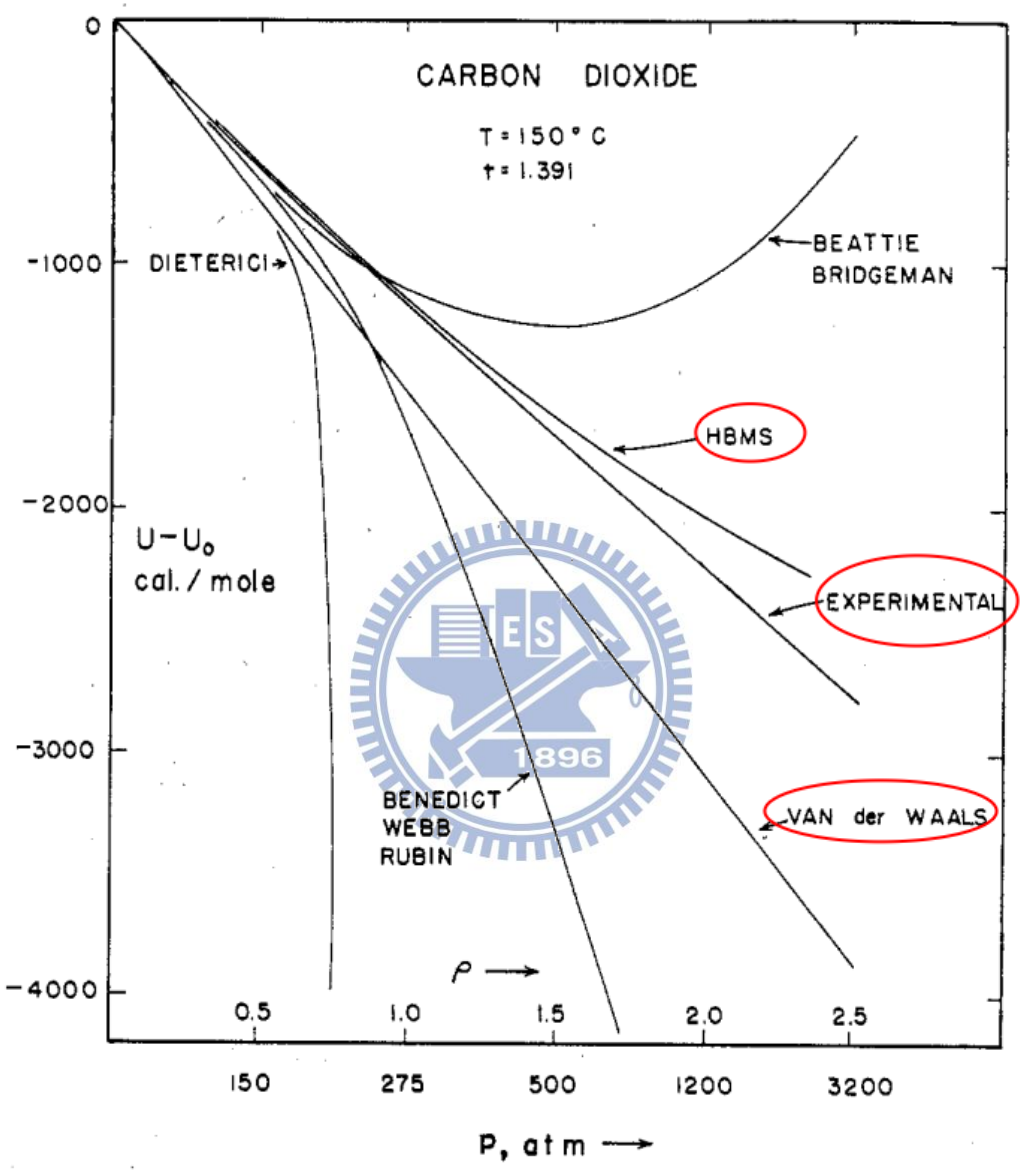

Fig.2-1 Comparison of equation of state with experiment for the internal energy excess function of carbon dioxide calculated along the isothermal line [6]

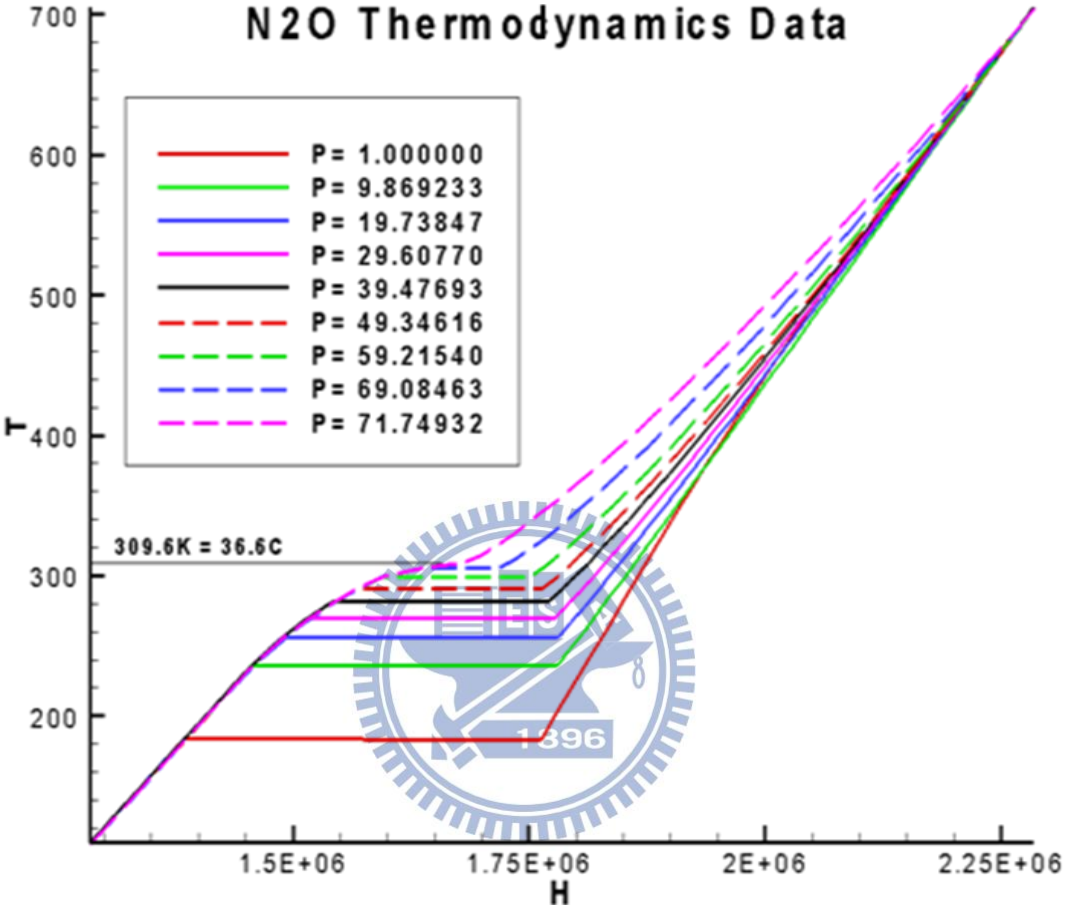

Fig.2-2 Nitrous oxide thermodynamic data [6]

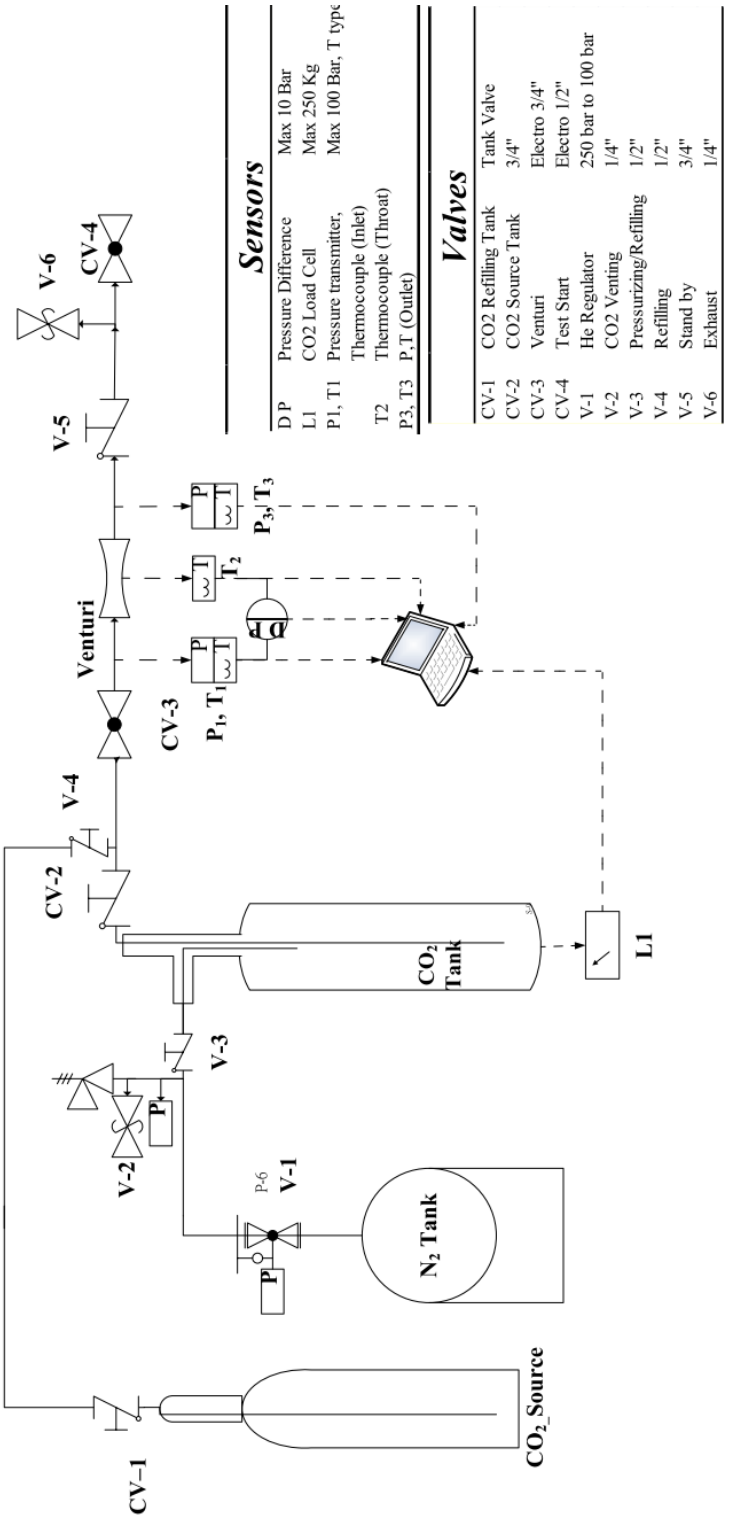

Fig. 3-1 Schematic of pipe and instruments diagram

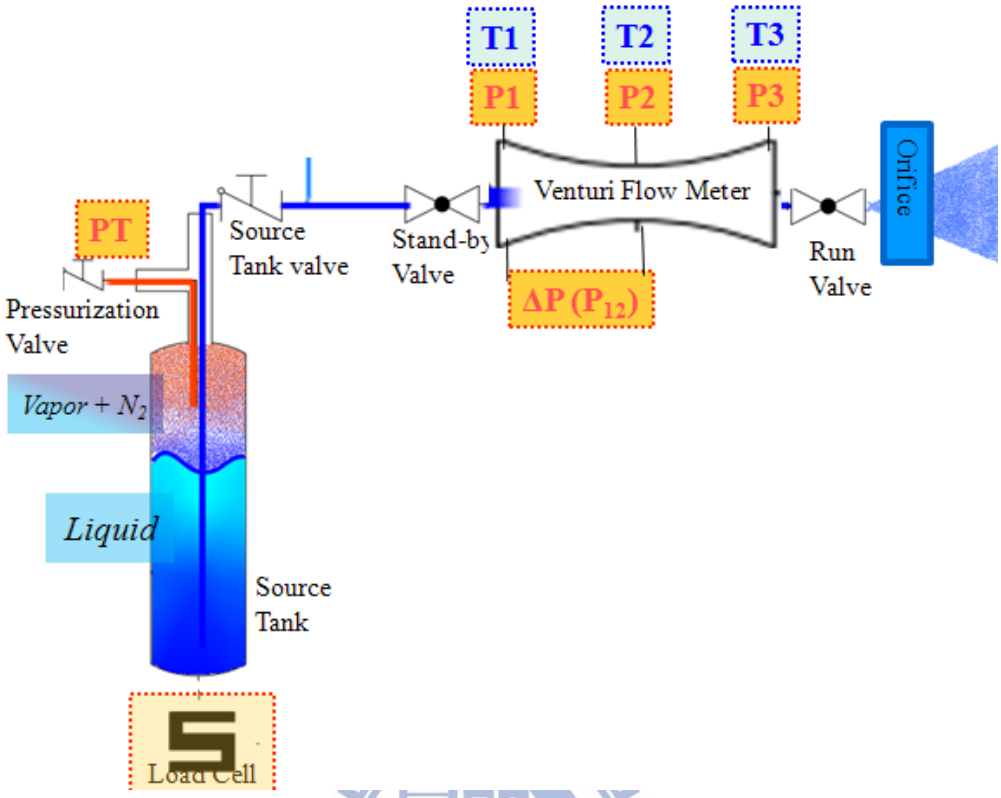

Fig. 3-2 Schematic of experimental instruments

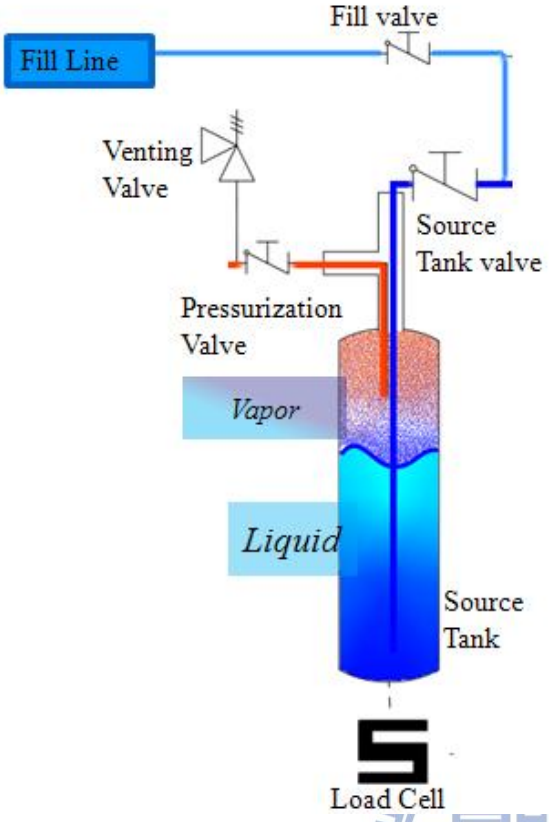

Fig. 3-3 Schematic of flow feeding system when filling mode

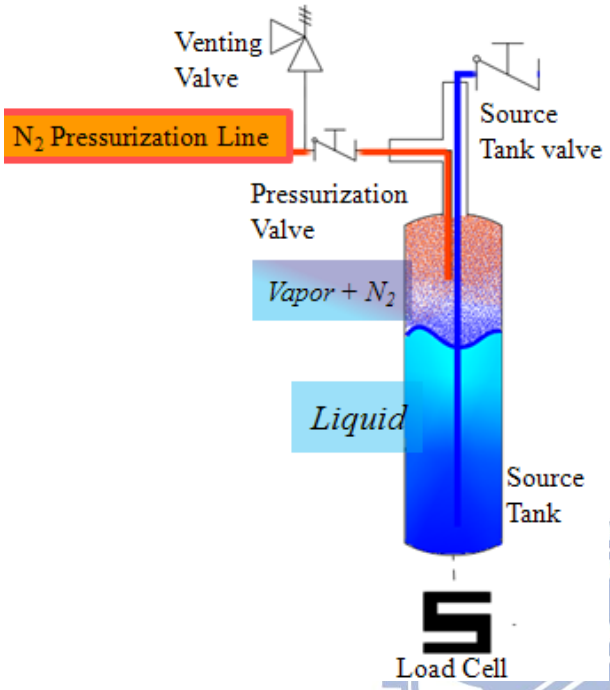

Fig. 3-4 Schematic of flow feeding system when pressurizing mode

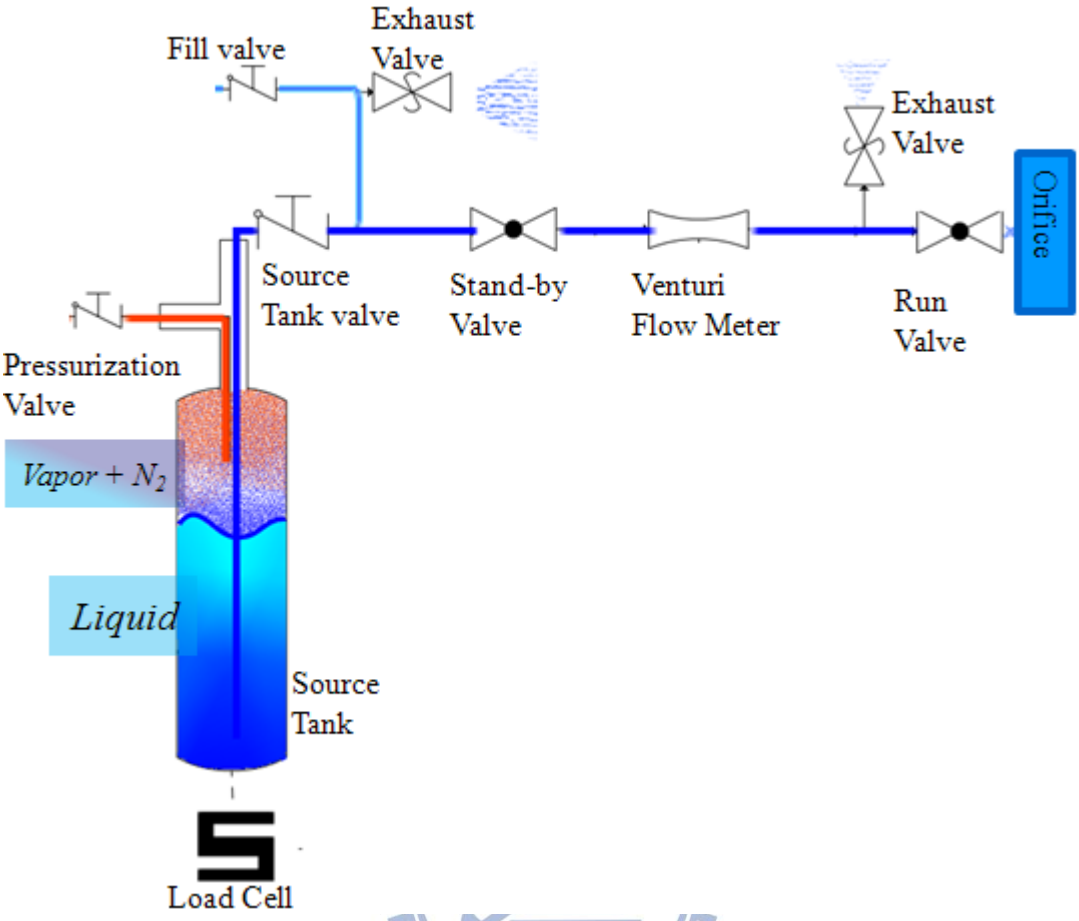

Fig. 3-5 Schematic of flow feeding system when stand-by mode

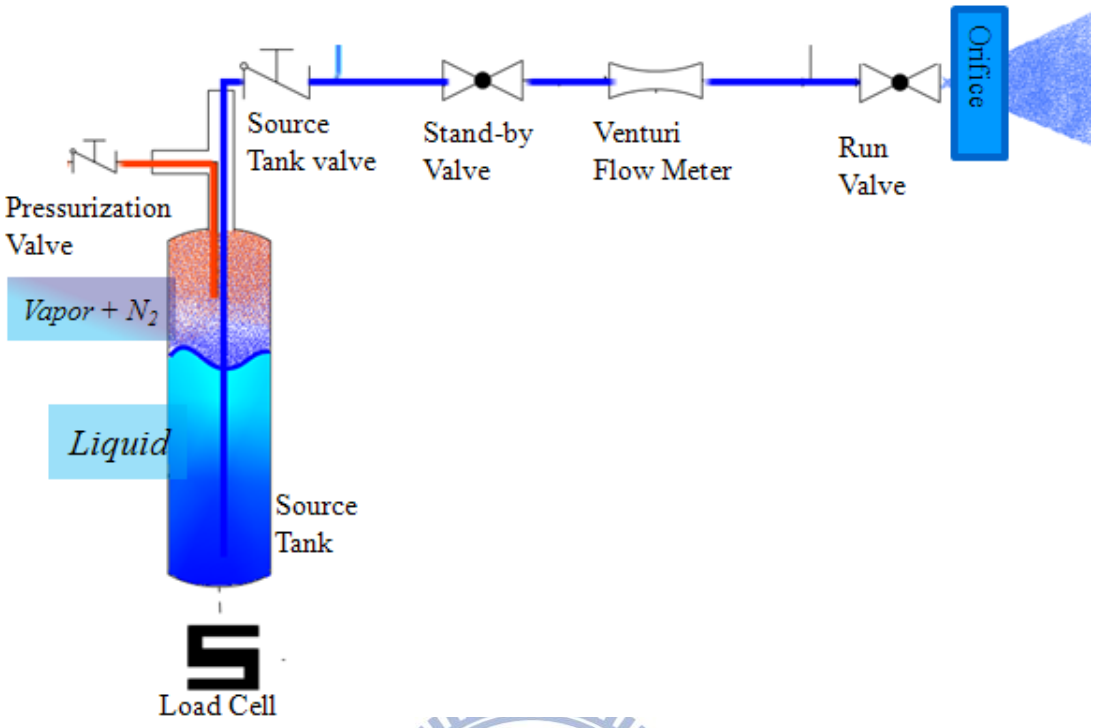

Fig. 3-6 Schematic of flow feeding system when run mode

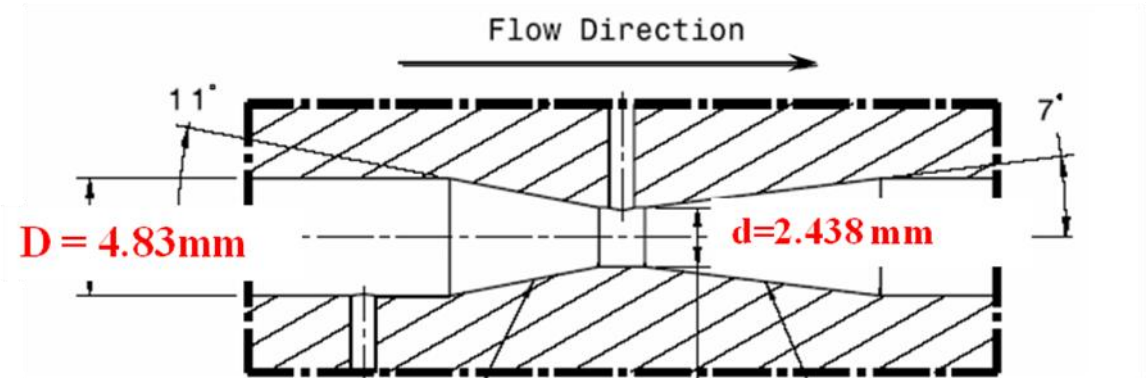

Fig. 4-1 Schematic of benchmark case utilized venturi [5]

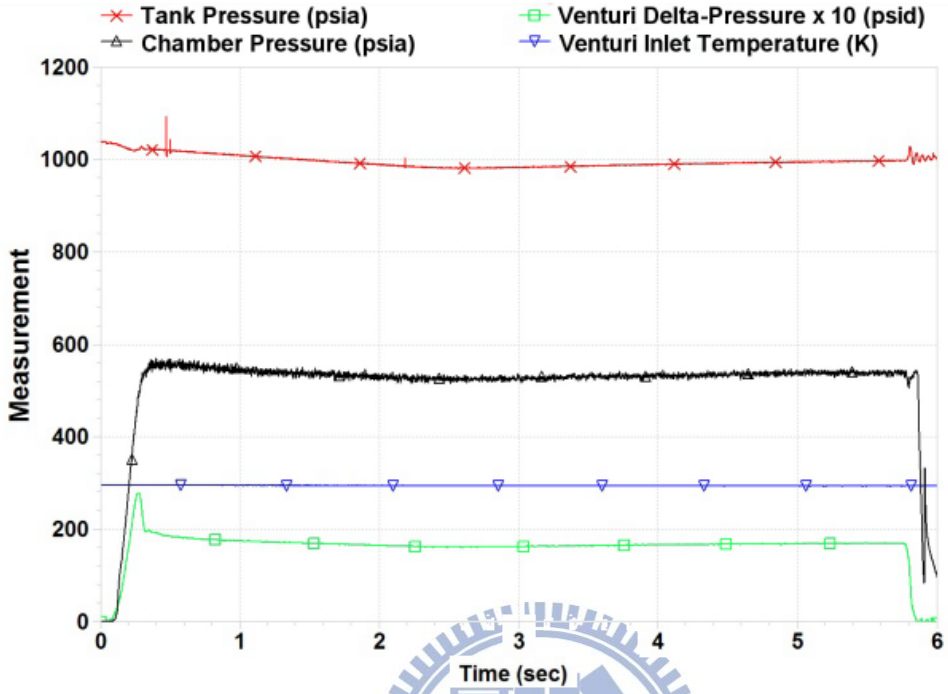

Figure 10. Pressure-time Trace for Hot Fire Test #30

Fig. 4-2 Experimental measurement vs. time for benchmark case [5]

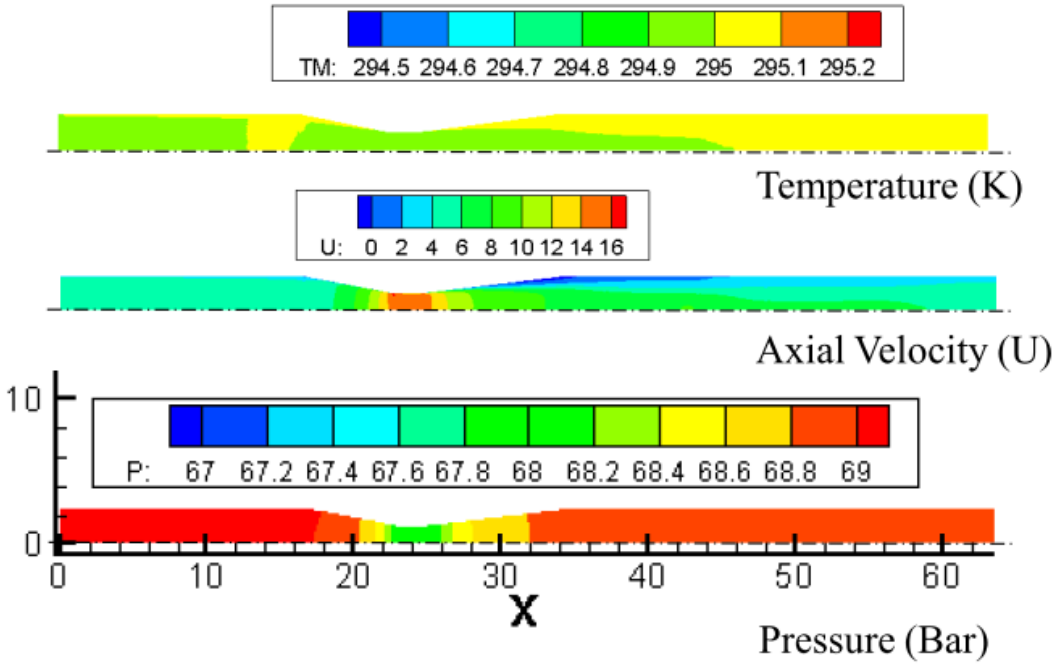

Fig. 4-3 Simulation results for benchmark case venturi, simulation result pressure difference P_{12} is 1.09 bar [5]

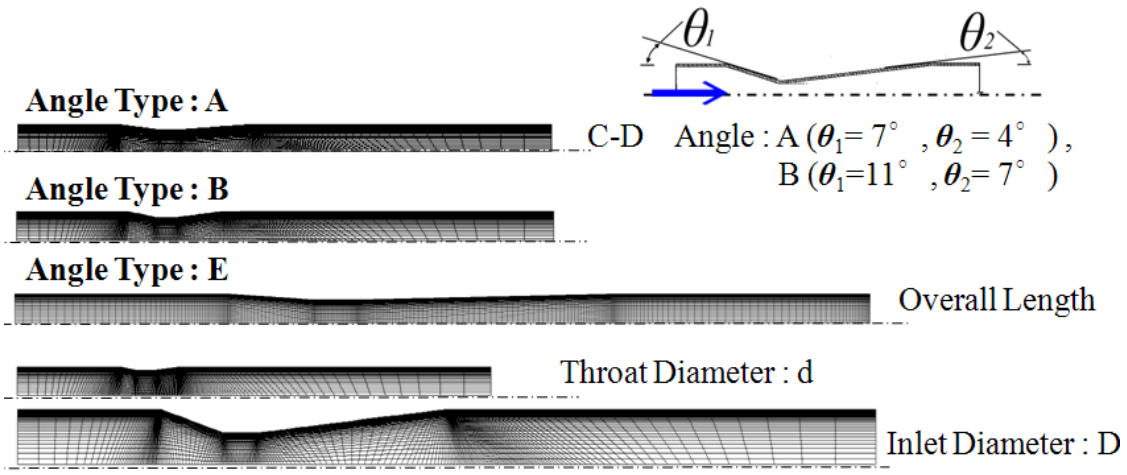

Fig. 4-4 Constructed mesh geometries and variation factors, including Converge-Diverge Angle (A, B), Overall Length Extended (E), throat diameter (d = 8mm, 9mm), Inlet Diameter (D = 10mm, 28mm)

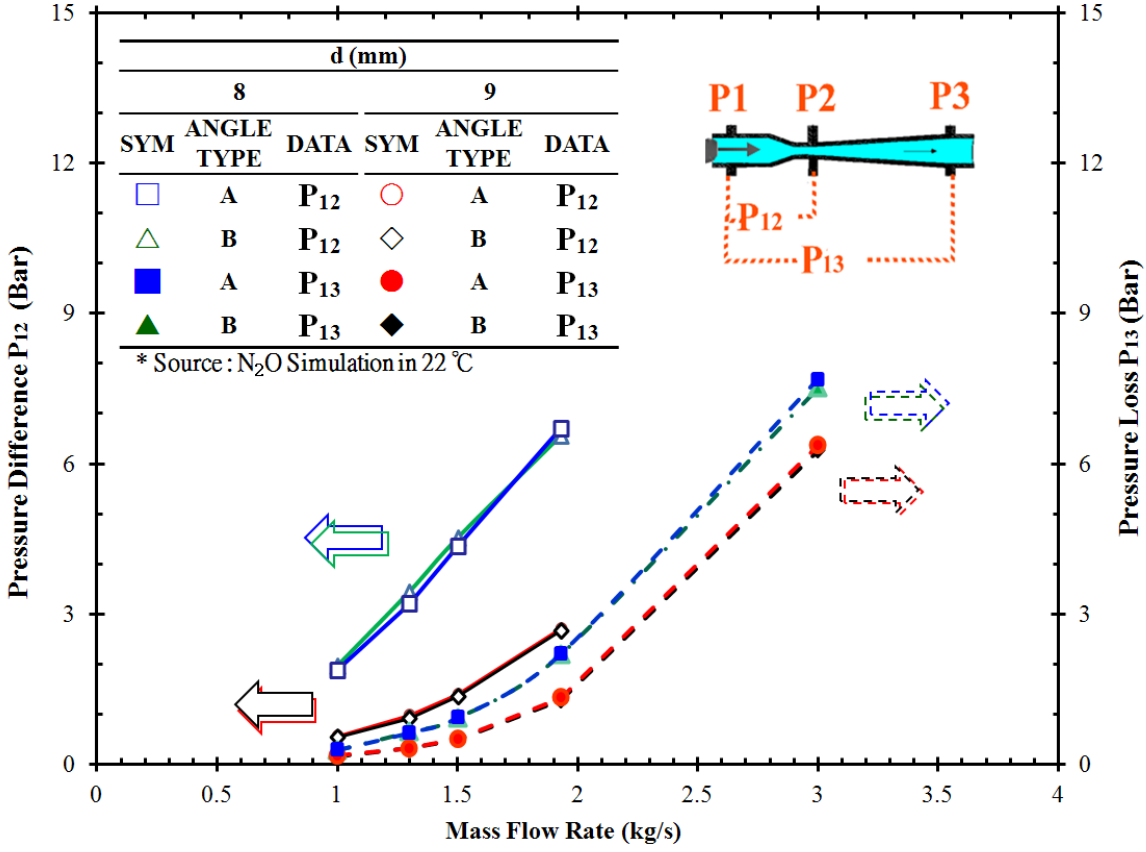

Fig. 4-5 Simulation result of 10 mm venturi with different throat diameter and expand angle

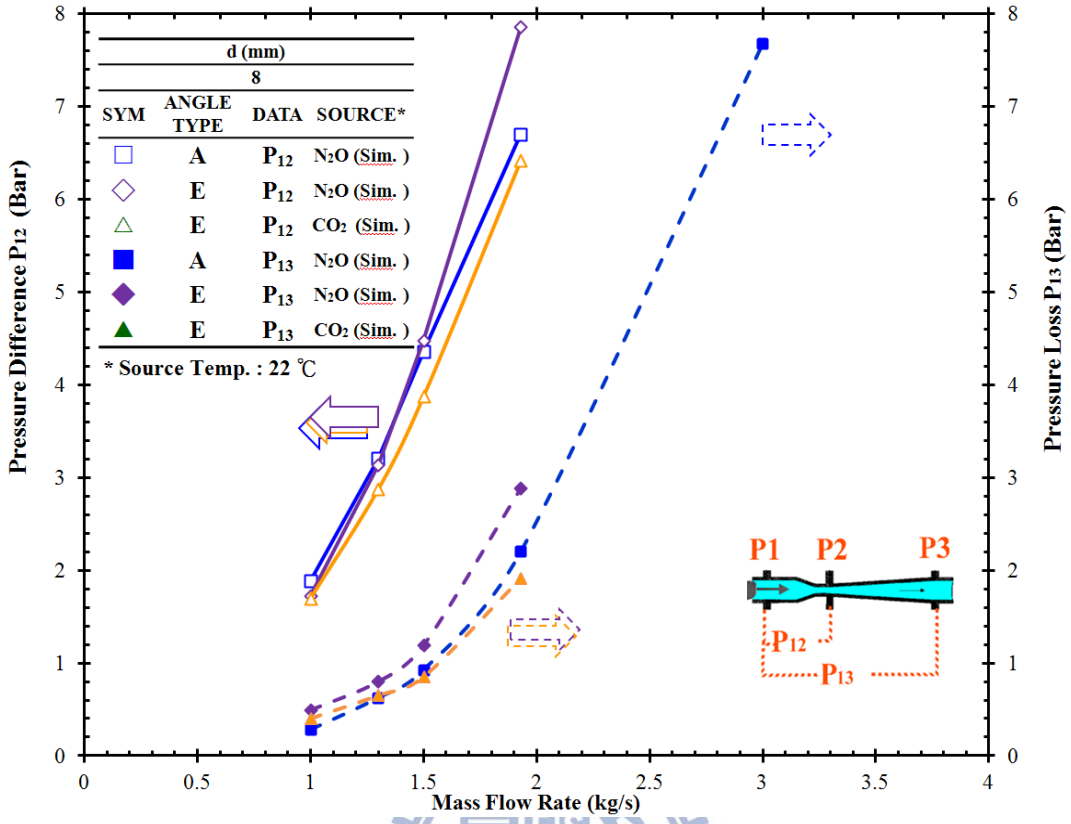

Fig. 4-6 Simulation result of 10 mm venturi with extended length and CO_2 data

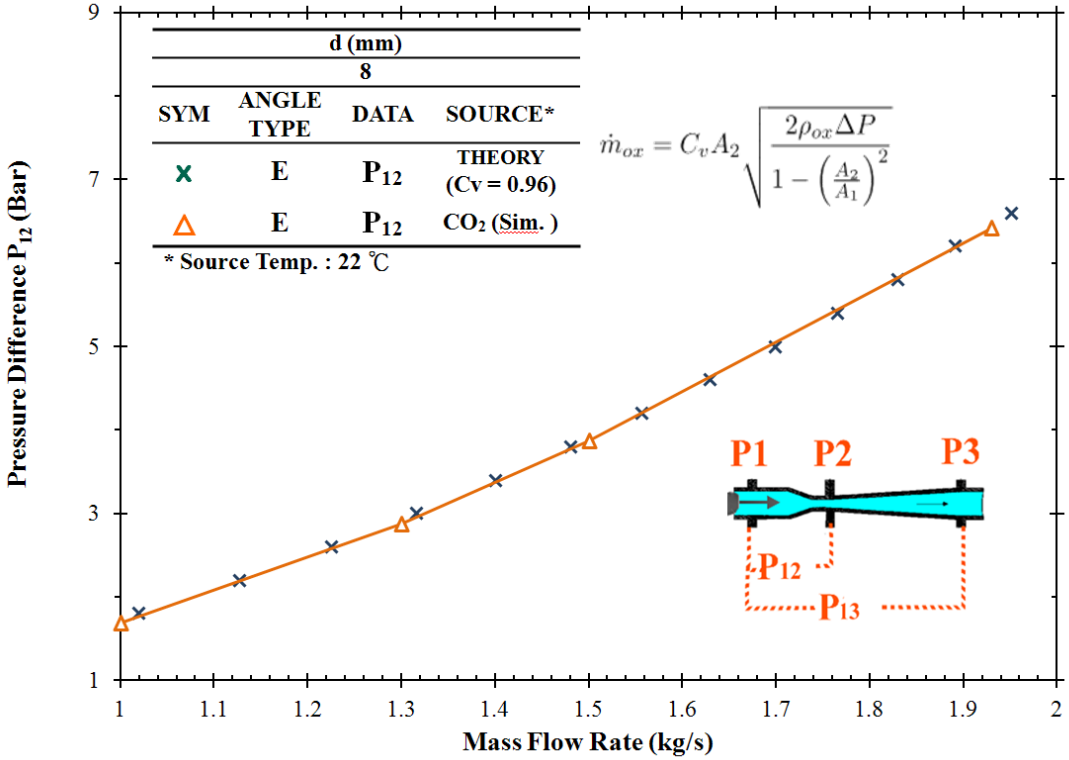

Fig. 4-7 Comparison between simulation and calculation result of 10 mm venturi

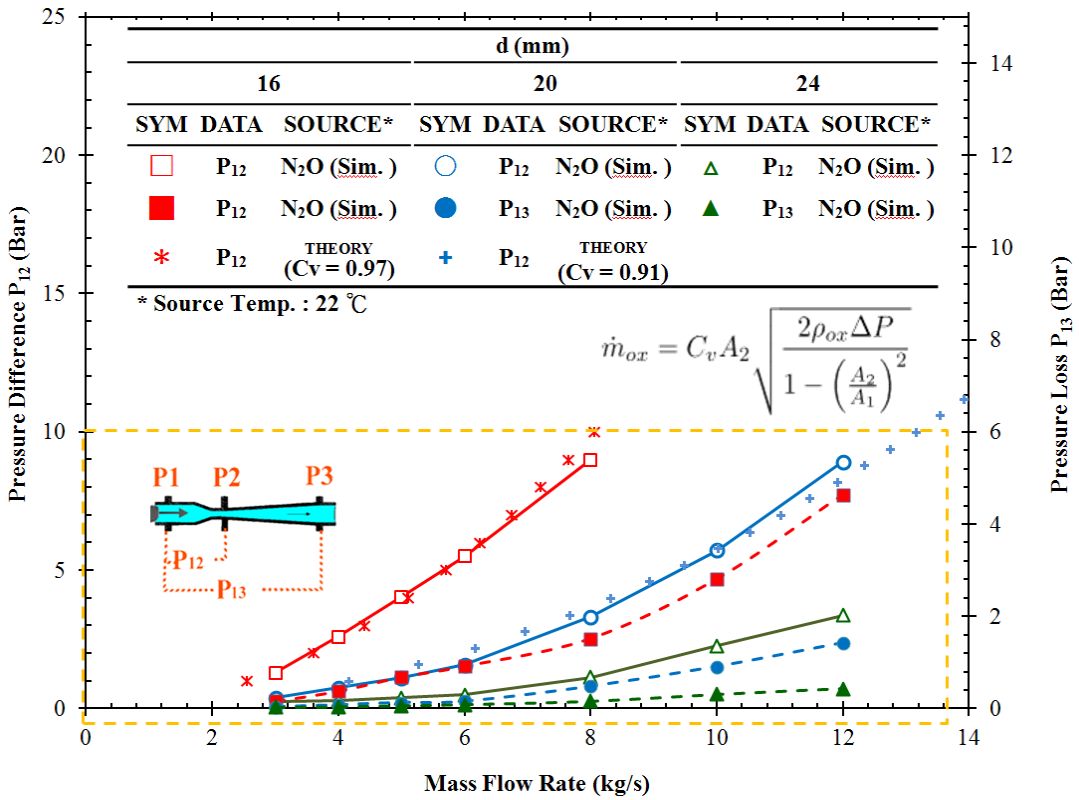

Fig. 4-8 Simulation and calculation result for 28 mm venturi

`

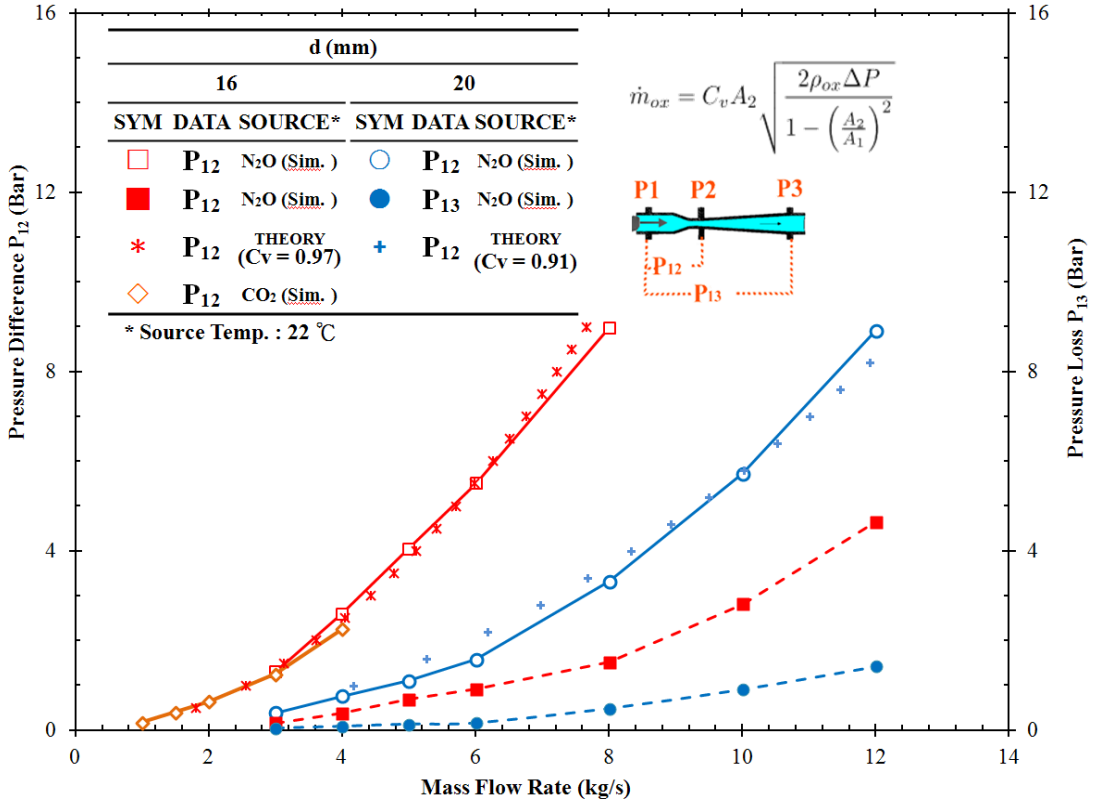

Fig. 4-9 Simulation and calculation result for 28 mm venturi with CO_2 simulation data

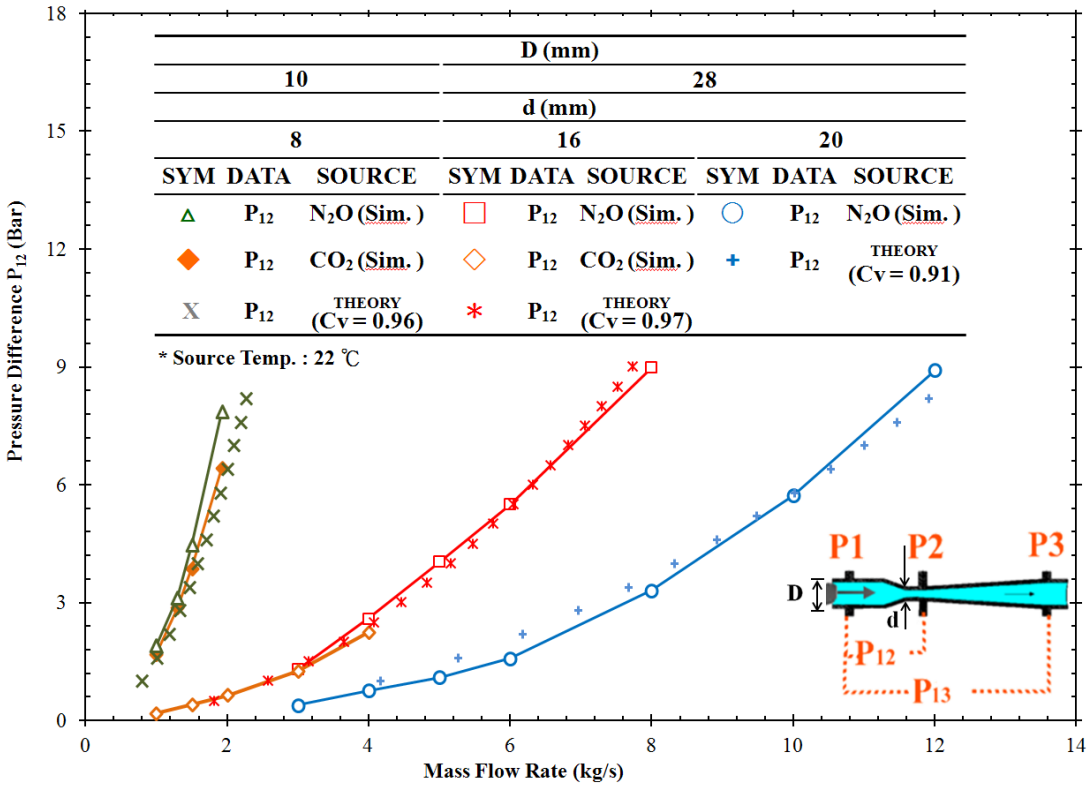

Fig. 4-10 Overall simulation results in comparison with Bernoulli eqn. theory results

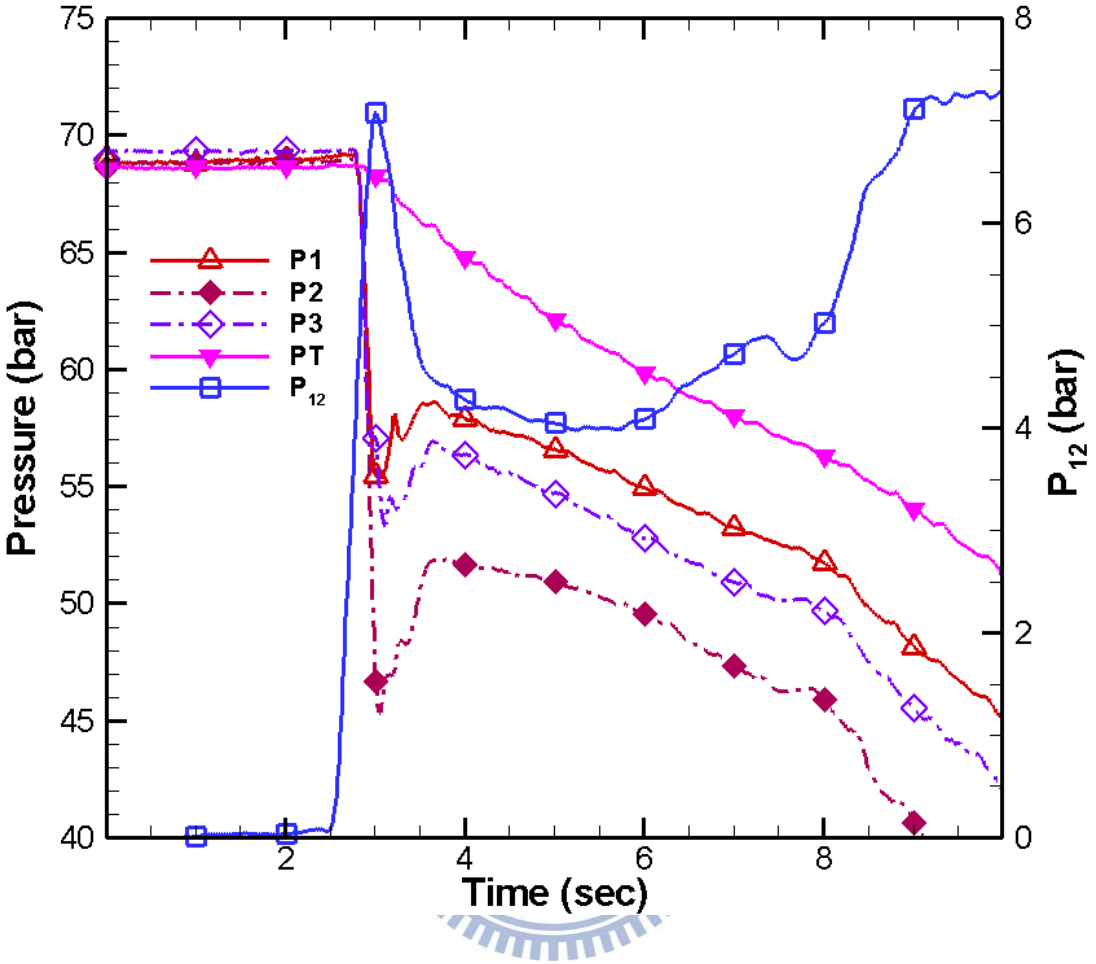

Fig. 4-11 Overall pressure transducers measured pressure data as a function of time for test case #1

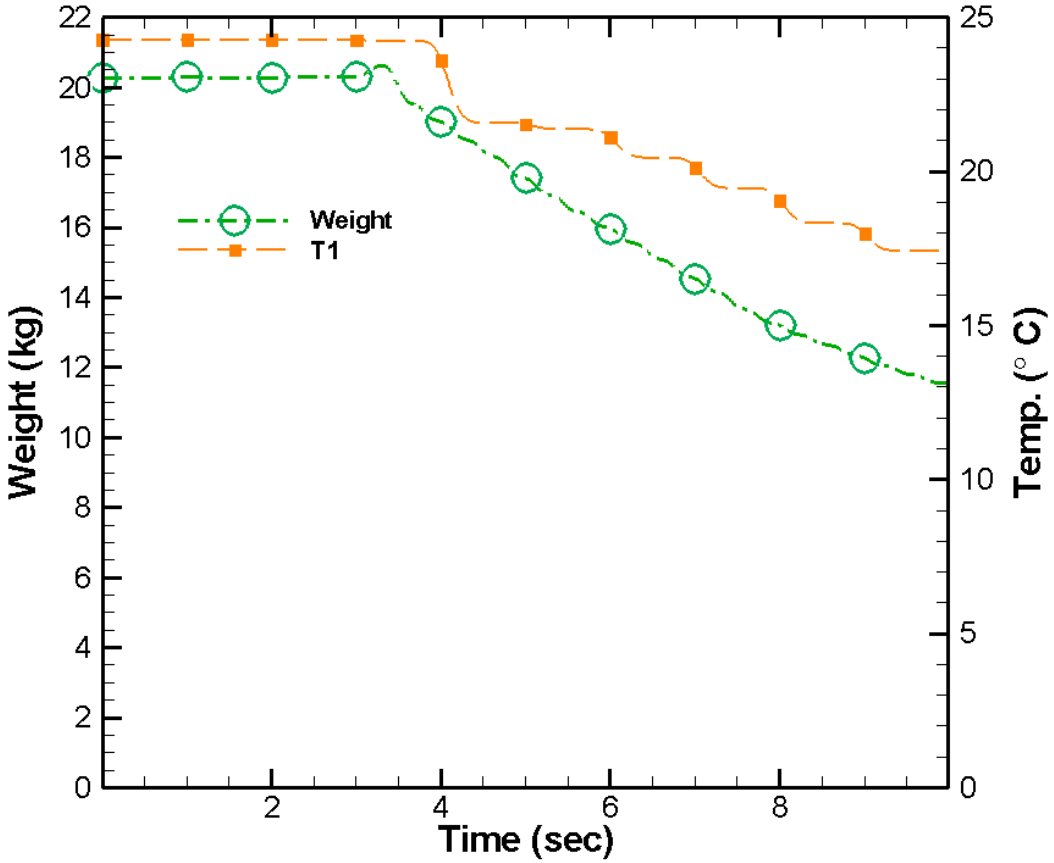

Fig. 4-12 Thermocouple and load cell data for test case #1

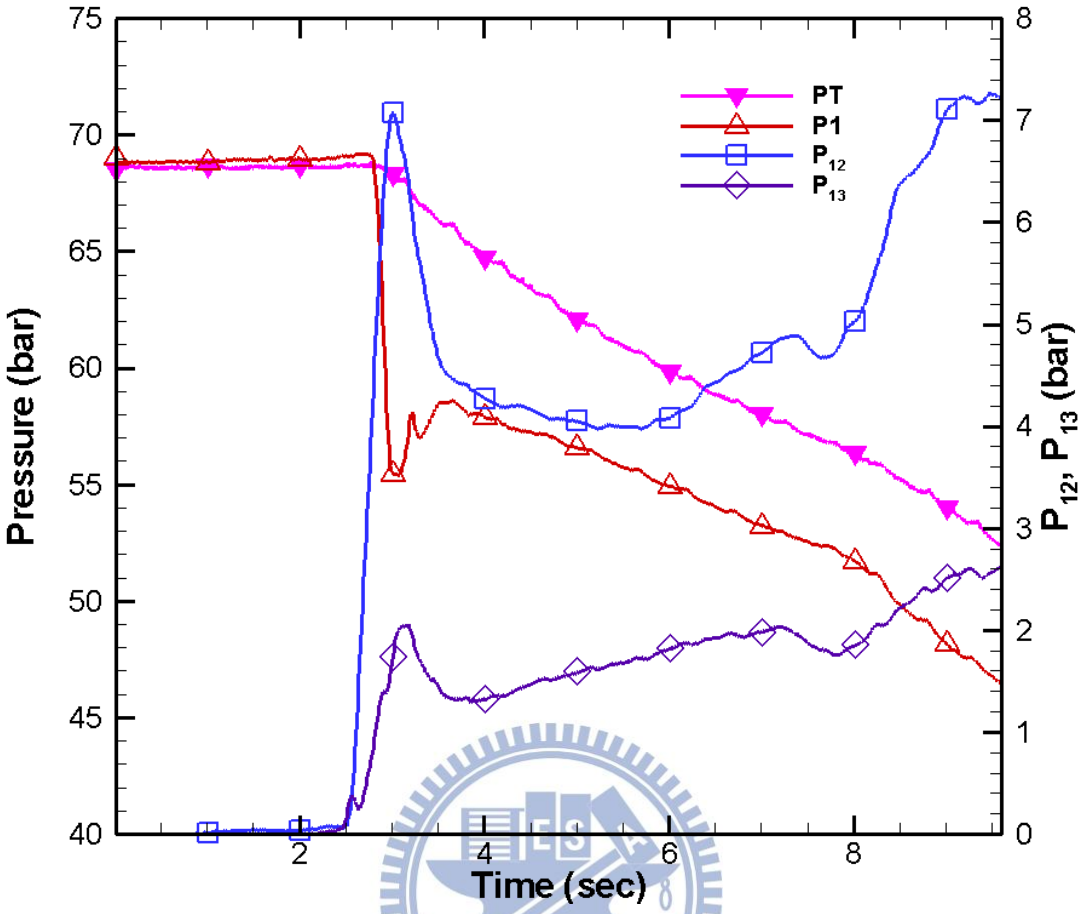

Fig. 4-13 Example of transferring P3 to P_{13} along with other pressure data as a function of time for test case #1

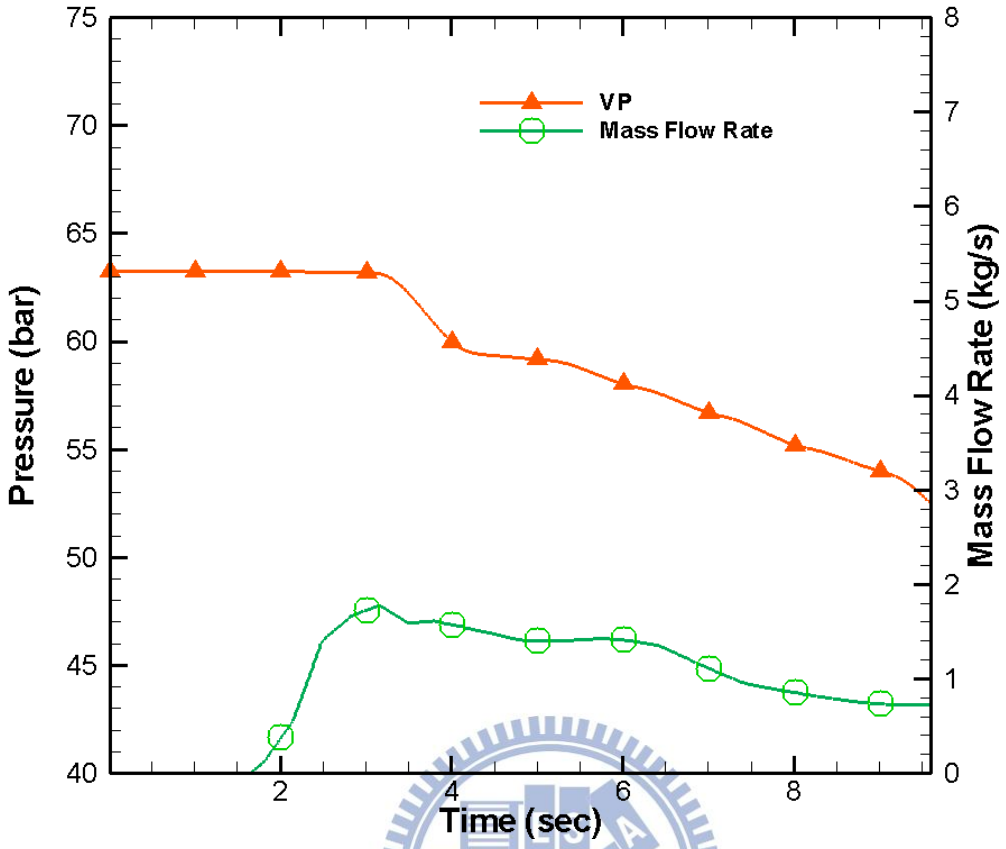

Fig. 4-14 Vapor pressure and mass flow rate data as a function of time for test case #1

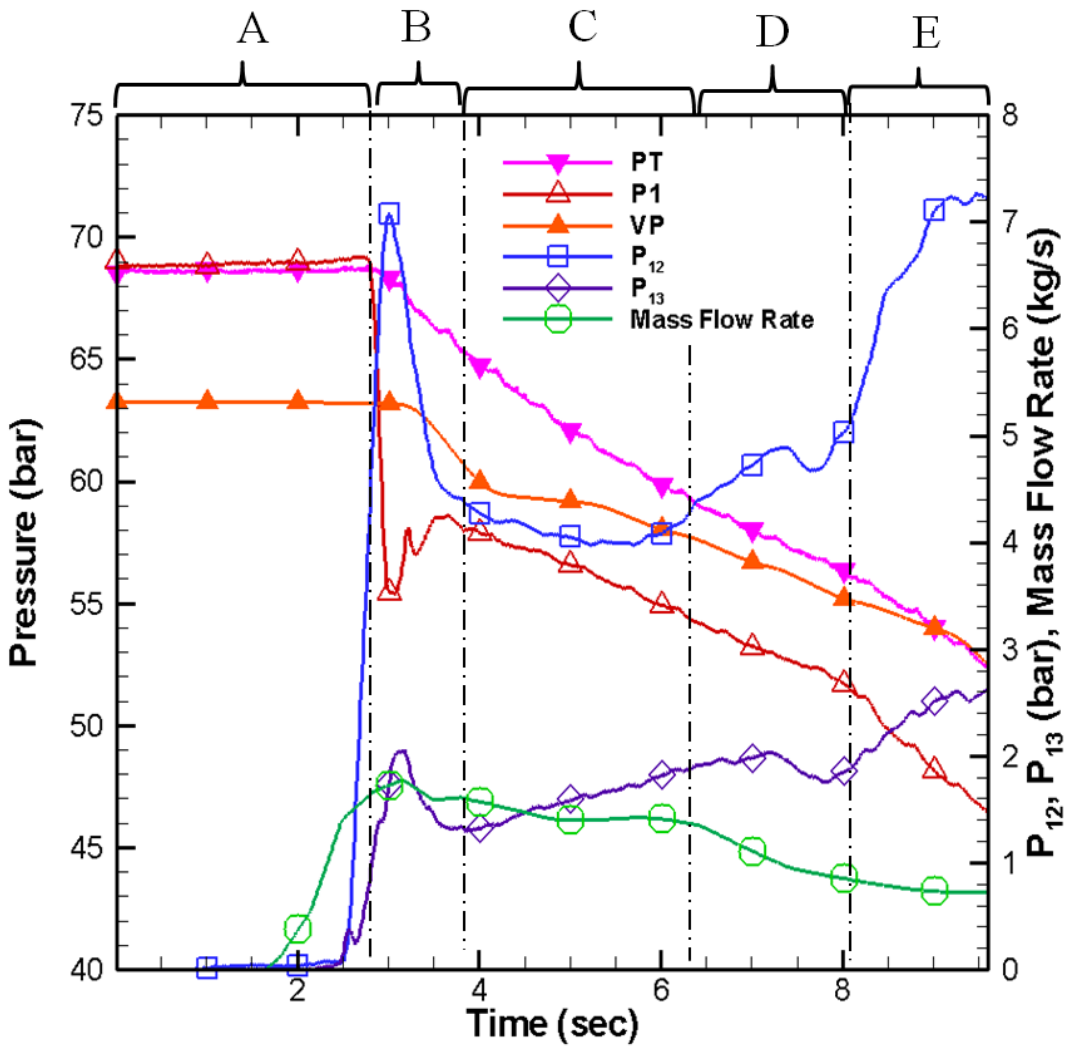

Fig. 4-15 Measurement data as a function of time for test case #1

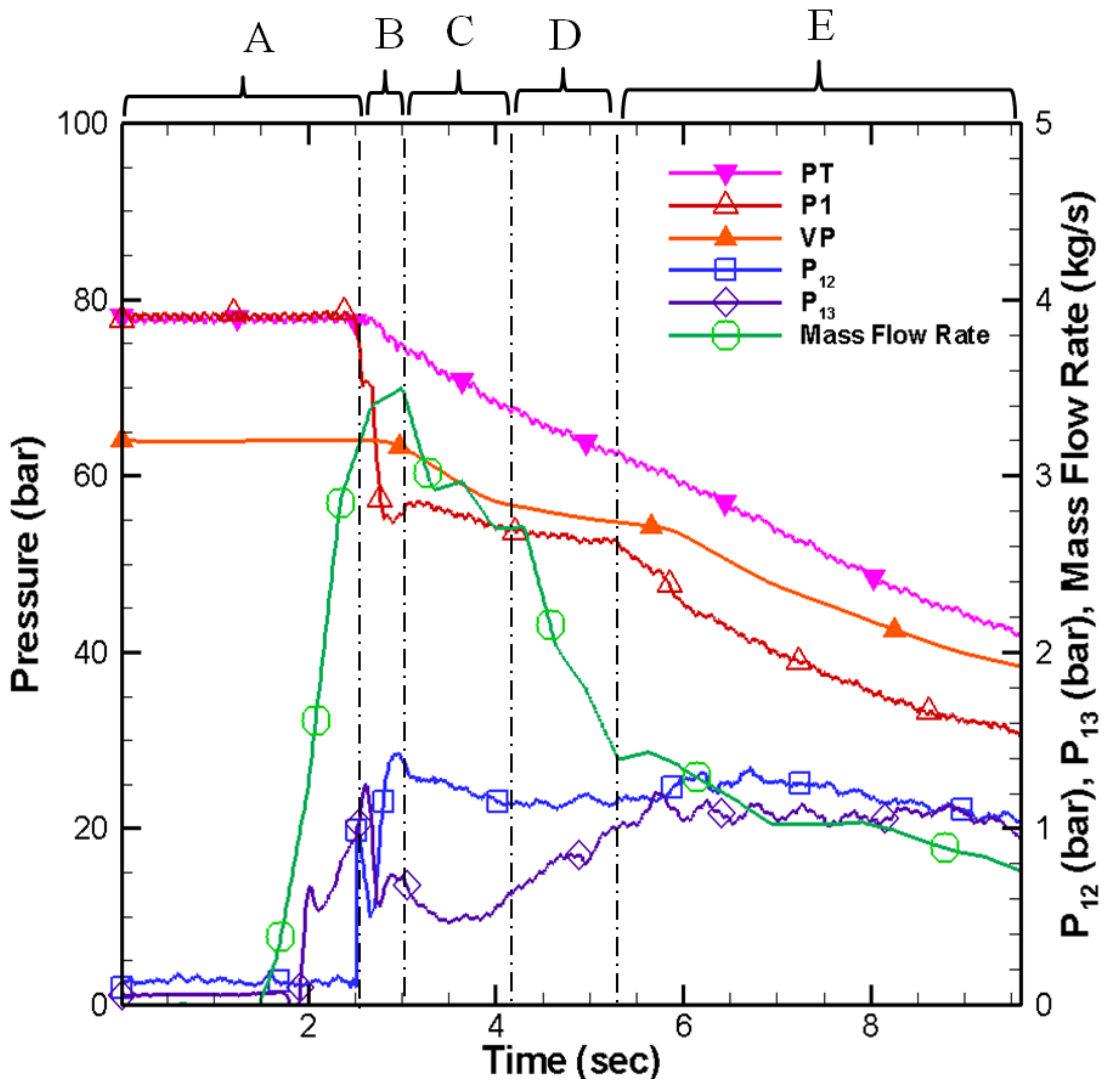

Fig. 4-16 Measurement data as a function of time for test case #2

Fig. 4-17 Measurement data as a function of time for test case #3

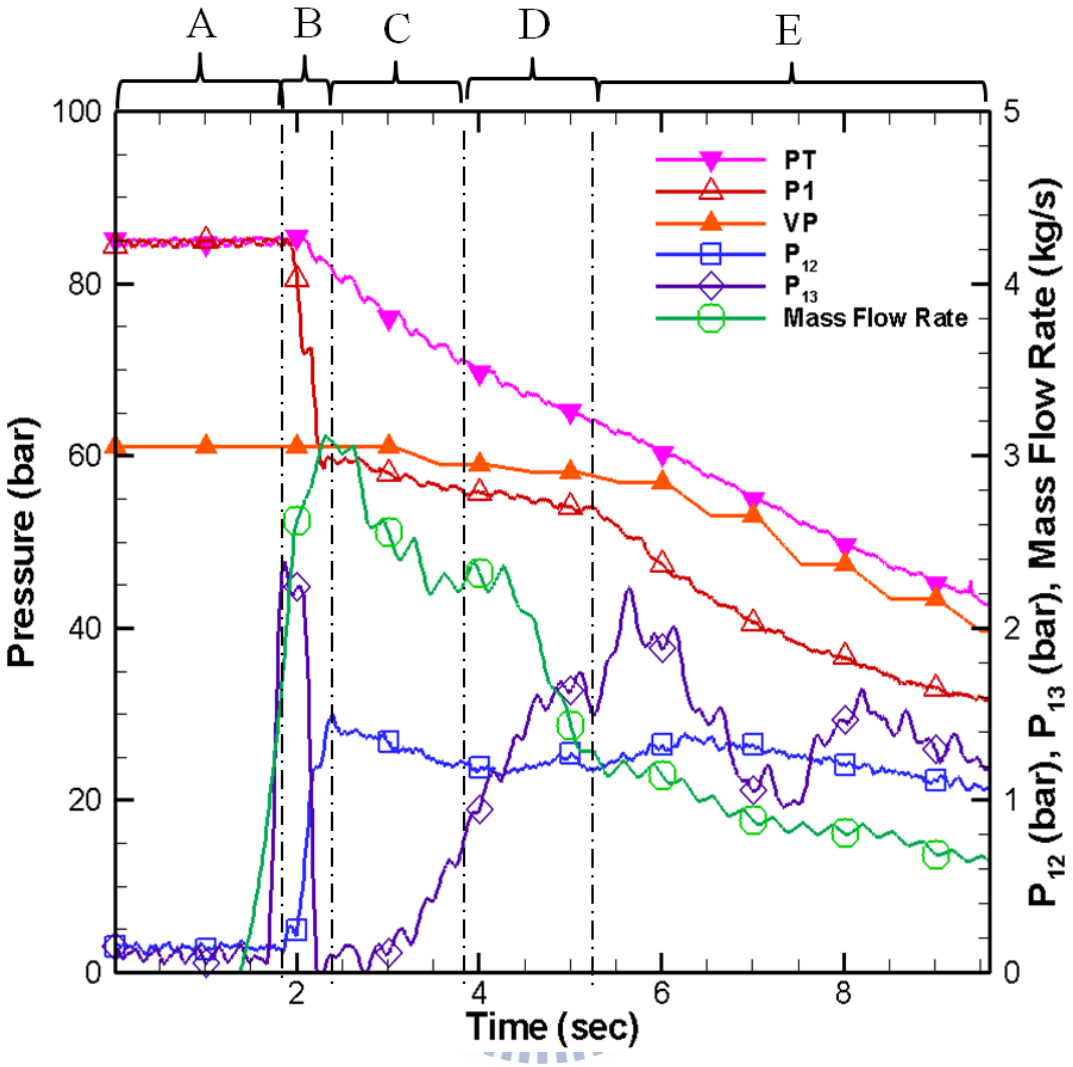

Fig. 4-18 Measurement data as a function of time for test case # 4

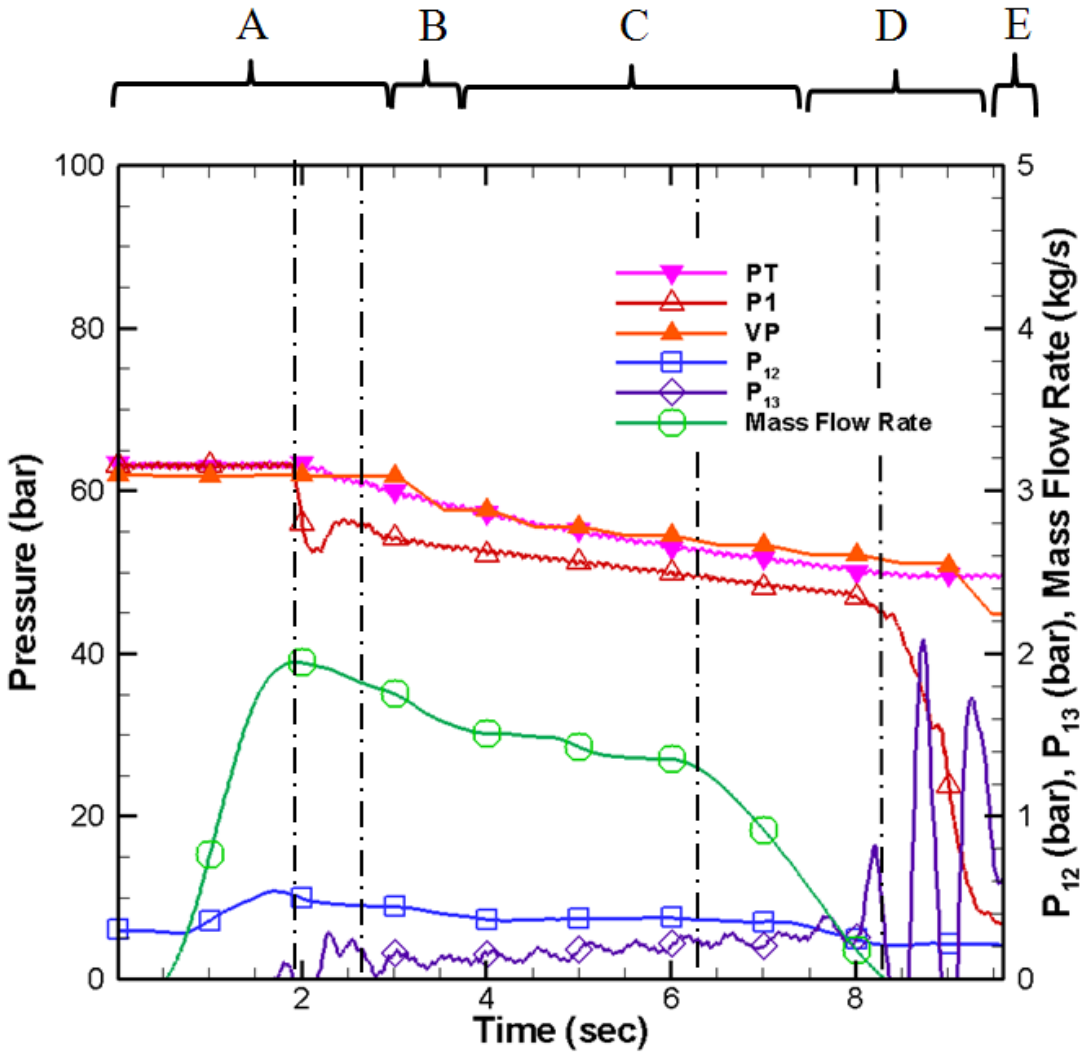

Fig. 4-19 Measurement data as a function of time for test case #5

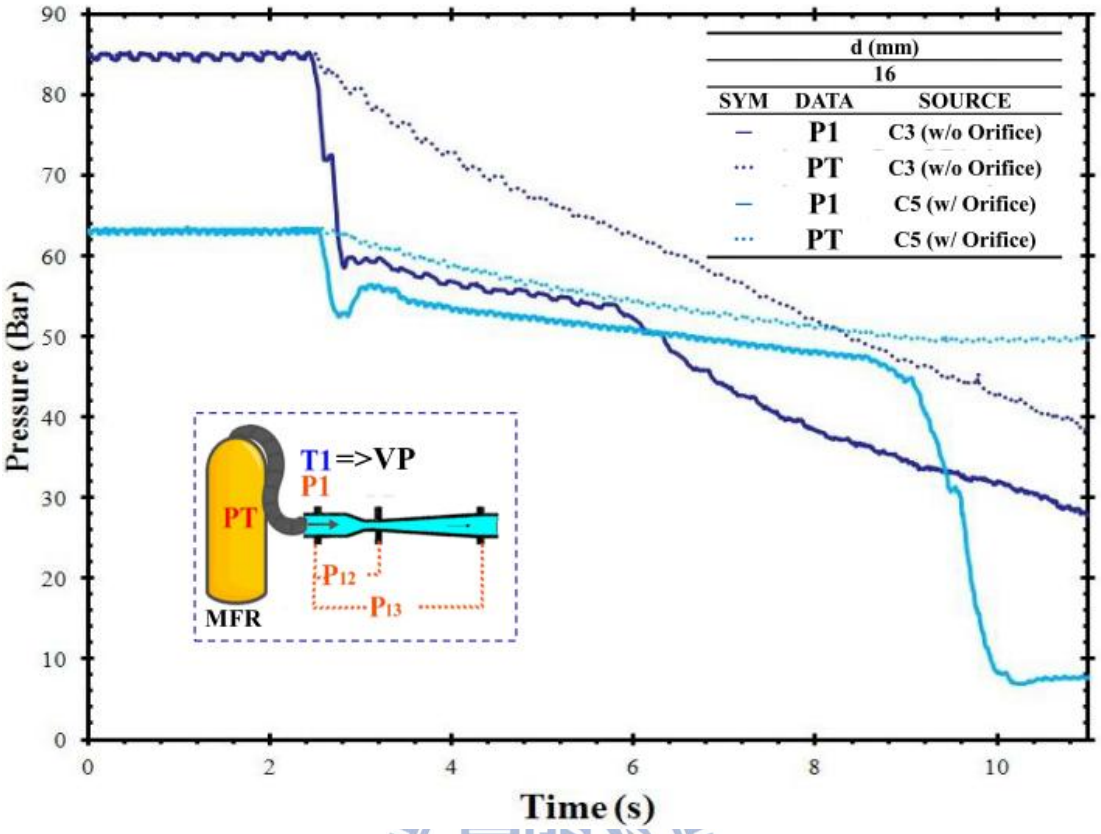

Fig. 4-20 Comparison of pressure drop range in cases with or without orifice

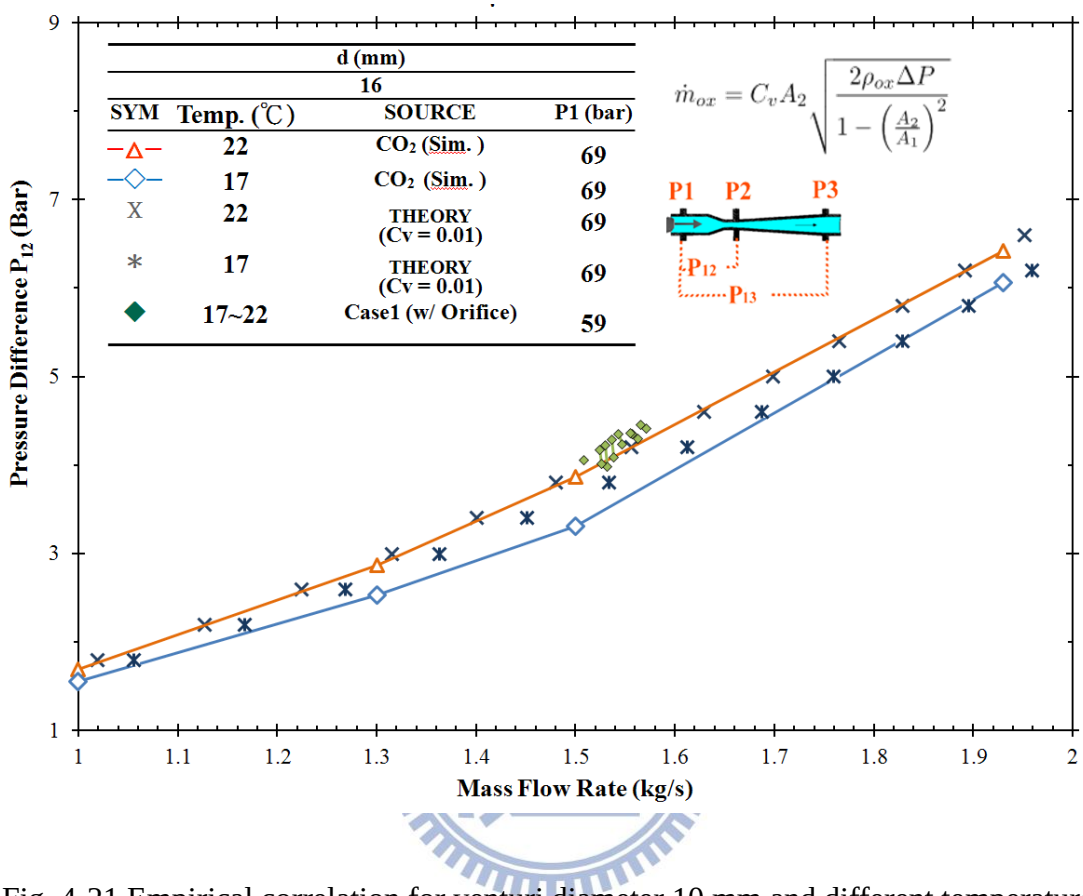

Fig. 4-21 Empirical correlation for venturi diameter 10 mm and different temperature

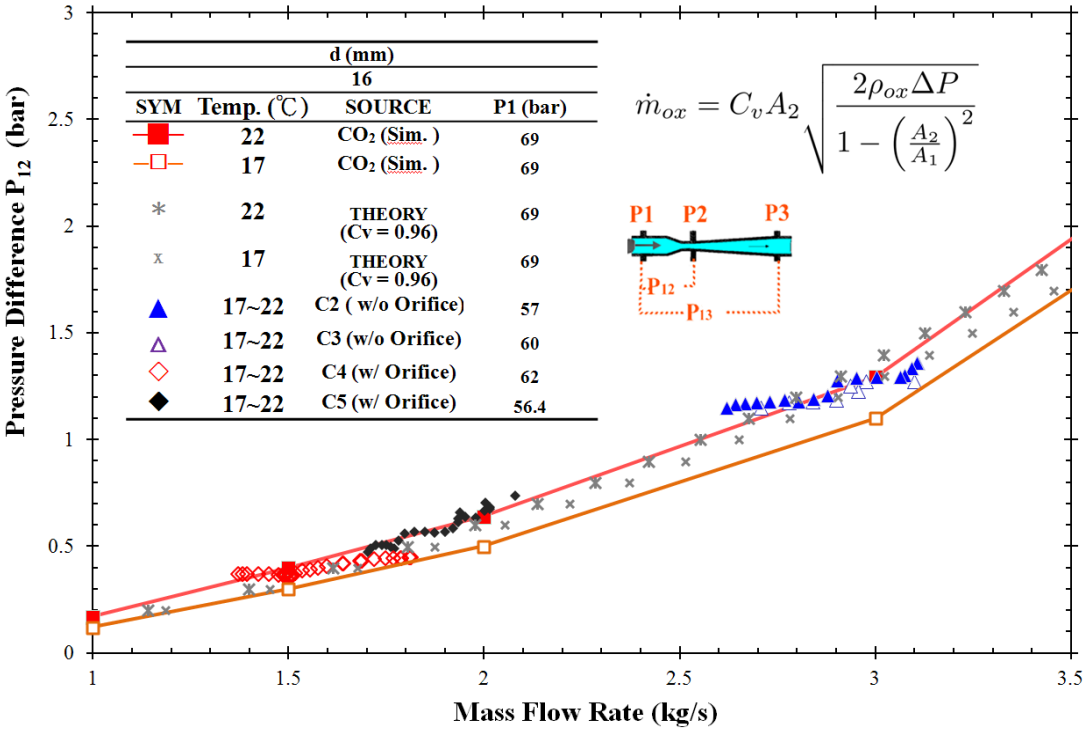

Fig. 4-22 Empirical correlation for venturi diameter 10 mm and different temperature